Mon. Not. R. astr. Soc. (1984) **208,** 721–750

The dynamical stability of differentially rotating discs with constant specific angular momentum

J. C. B. Papaloizou *Theoretical Astronomy Unit, School of Mathematical Sciences, Queen Mary College, London E1 4NS*

J. E. Pringle *Institute of Astronomy, Madingley Road, Cambridge CB3 0HA*

Received 1983 August 10

Summary. We investigate the dynamical stability of a differentially rotating disc (or torus) of fluid of uniform entropy and uniform specific angular momentum. Such a fluid is neutrally stable to axisymmetric perturbations. In this paper we consider non-axisymmetric perturbations and undertake a global stability analysis. We present a general study of the normal mode eigenvalue problem and the explicit analytic solution of a pair of particular limiting cases. We derive the fastest growing eigenmodes by numerical integration of the full linearized equations for more general cases. Our overall result is that the tori are unstable to low order non-axisymmetric modes and that the modes grow on a dynamical time-scale. We argue that because of the strength of the instability, similar unstable modes must exist in tori of non-uniform entropy or of non-uniform specific angular momentum.

1 Introduction

The study of differentially rotating systems is of importance in astronomy. Differential rotation is a major ingredient in models of galactic discs (Toomre 1977) and accretion discs (Pringle 1981). It plays a role in solving the excess angular momentum problem in the dynamics of star formation, and must occur even in originally uniformly rotating stars as they evolve, through redistribution of mass with radius, through tidal interaction with a companion (Savonije & Papaloizou 1983) or through the accretion of high angular momentum material from a companion (Kippenhahn & Thomas 1978).

In this paper we concentrate our attention on the thick accretion discs, or accretion tori, which are invoked in accretion type models of quasars. Such models are required, rather than the standard thin discs, when the accretion luminosity approaches the Eddington limit (Shakura & Sunyaev 1973) or when inefficient cooling forces the disc to become so hot that the local gas sound speed approaches the circular velocity and the disc thickness becomes comparable to, or greater than, the radius. Such tori are also constructed in an effort to produce a configuration which might be conducive to the formation of jets, using the empty vortex region along the accretion axis (Lynden-Bell 1978).

As pressure forces play a role in the equilibrium structure of such tori, there is no reason for the rotation law to be Keplerian and it may be specified in an arbitrary manner. Because of this freedom, it is essential to know whether the requirement of dynamical stability imposes any constraints on the rotation law.

There is no complete theory for the stability of differentially rotating systems (see for example Toomre (1969), and the relevant chapters in Tassoul (1978)). For a rotating, homentropic gas the only stability criterion available is that due to Rayleigh (1916) which states that a necessary (but not necessarily sufficient) criterion for stability is that the specific angular momentum should not decrease outwards. This is the only criterion used so far in the literature for limiting the range of allowable models (e.g. Abramowicz, Calvani & Nobili 1980). Moreover, it is generally assumed, either explicitly or implicitly, that the criterion is a sufficient one and, in particular, that models with constant specific angular momentum, are dynamically stable. For example Madej & Paczynski (1977) argue that in the outer regions of an accretion disc in a close binary system there is a 'dynamical instability which tends to keep the angular momentum per unit mass constant with radius'. In their paper on the evolution of accretion tori, Abramowicz, Henderson & Ghosh (1983) assume that the time-scale of evolution is much longer than the dynamical time-scale.

However, Rayleigh's criterion is derived from a consideration of axisymmetric modes, and indeed for such modes it is both necessary and sufficient. The properties of non-axisymmetric modes are still essentially unknown, and the theory for these is much more complex. It is not possible in the non-axisymmetric case to derive an energy principle which gives necessary and sufficient conditions for stability. In addition, methods of analysis discussed in the literature, such as the tensor virial method or local stability analysis, do not provide sufficient conditions for stability to non-axisymmetric modes. In the case of the tensor virial method or other adapted trial function methods, there is no guarantee that any derived instabilities are genuine (Friedman & Schutz 1978). Thus the results of Hacyan (1982) who used such an approach in a study of the stability of accretion tori are inconclusive. A local stability analysis can be used to make a case for instability, but of course in this case the criterion derived is simply the Rayleigh criterion (e.g. Abramowicz *et al.* 1984).

This paper is the first to emerge from our study of the non-axisymmetric modes of differentially rotating discs. To study such modes it is essential to solve the time-dependent linearized fluid equations and so to undertake a global stability analysis. In view of such well-known features as corotation singularities, one may not, in general, assume *a priori* that discrete modes exist. The results of such a study should throw light on the stability of differentially rotating flows in general, and in particular of all disc flows as well as accretion tori. In this paper we limit ourselves to a study of non-self-gravitating, homentropic tori with constant specific angular momentum because in this case the stability problem is greatly simplified.

We approach the problem of the stability of such tori in three different ways: a general study of the normal mode eigenvalue problem, the explicit analytic solution of a pair of particular limiting cases and the full numerical solution of the time-dependent linearized fluid equations for more general cases. The results from these approaches are interrelated and complementary and help to shed light on the nature of the instability. Our overall result is that all such tori are unstable to low order modes and that the instability occurs on a dynamical time-scale. At first sight this is surprising, as there is no self-gravity in the problem and the local analysis gives no hint of such instabilities. The instabilities are global and can only be definitively identified by a proper solution of the full equations.

In view of the interrelatedness of our results and of the fact that no simple instability

criterion emerges, we present our analysis in one rather lengthy paper. The structure of the paper is as follows. In Section 2 we display the equilibrium configurations, in general, and for the particular cases of the gravity being due to a central point mass and of the system having uniform specific angular momentum. In Section 3 we derive the linear perturbation equation for general polytropic equilibria and show how a local stability analysis gives rise to Rayleigh's criterion. In Section 4 we consider the perturbation analysis for constant specific angular momentum tori. We show that incompressible tori are stable and that finite compressibility has a destabilizing effect. We then discuss the general eigenvalue problem and show that the modes of oscillation of such tori are discrete. By considering an extended class of equilibria, we are able to illustrate, by means of a somewhat lengthy analysis, how the unstable modes arise. This analysis implies for any actual problem we are considering that at least modes with large values of m can be expected to be unstable. In Section 5 we present two explicit analytic examples of the instability. We consider a thin cylindrical shell and a thin isothermal torus. The similarity between these problems and the one discussed in Section 4 is evident and unstable modes are calculated for both. In Section 6 we calculate the fastest growing unstable modes in relatively distorted tori by direct numerical computation. We take some trouble to show that the instabilities we discover are not artefacts of the numerical methods employed. Our results and conclusions are summarized in Section 7.

2 The equilibrium configurations

2.1 GENERAL POLYTROPIC EQUILIBRIA

We consider the equilibrium configuration of a non-self-gravitating differentially rotating fluid. We use cylindrical polar coordinates (ϖ, ϕ, z) in an inertial frame and assume that the rotation is about the z axis. The equilibrium equation for a fluid subject to an external potential ψ is

$$-\frac{1}{\rho}\nabla p - \nabla\psi + \Omega^2\varpi\hat{\boldsymbol{\varpi}} = 0 \tag{2.1}$$

where p is the pressure, ρ the density, Ω the angular velocity and $\hat{\boldsymbol{\varpi}}$ the unit vector in the radial direction. Throughout most of this paper we assume the external potential as due to a gravitating point mass, M, situated at the origin, so that $\psi = \psi_p$ where

$$\psi_p = -GM/(\varpi^2 + z^2)^{1/2}. \tag{2.2}$$

We also assume the equation of state of the fluid to be that of a polytrope, that is

$$p = A\rho^{1+1/n} \equiv A\rho^{\gamma}, \tag{2.3}$$

where A is the polytropic constant and n the polytropic index. For this equation of state we require $\partial\Omega/\partial z = 0$ (see, e.g. Tassoul 1978). Thus we take Ω to be a function of ϖ alone and define a rotational potential ψ_{rot} so that

$$\frac{\partial\psi_{rot}}{\partial\varpi} = -\Omega^2\varpi. \tag{2.4}$$

By combining the above equations we may reduce the equilibrium condition to

$$\nabla[\psi_{rot} + \psi + (n+1)p/\rho] = 0 \tag{2.5}$$

where we note that $(n+1)p/\rho = \int dp/\rho$ is the specific enthalpy. It follows that

$$(n+1)p/\rho + \psi + \psi_{rot} = C = \text{const.} \tag{2.6}$$

The constant, C, defines the boundary of the configuration. If the fluid extends to the surface on which $p = \rho = 0$ then the surface is given by

$$\psi + \psi_{\rm rot} = C. \tag{2.7}$$

2.2 CONFIGURATIONS WITH CONSTANT SPECIFIC ANGULAR MOMENTUM

If the angular velocity $\Omega \propto \varpi^{-2}$, then the specific angular momentum $h \equiv \varpi^2\Omega$ is constant. In this case we find from equation (2.4) that $\psi_{\rm rot} = h^2/(2\varpi^2)$, where we have taken the constant of integration so that $\psi_{\rm rot}$ vanishes as $\varpi \to \infty$. When ψ is given by equation (2.2), so that the external field is produced by a point mass at the origin, the equilibrium equation (2.6) becomes

$$\frac{p}{\rho} = \frac{1}{(n+1)}\left(\frac{GM}{(\varpi^2+z^2)^{1/2}} - \frac{h^2}{2\varpi^2} + C\right). \tag{2.8}$$

To specify the equilibria it is convenient to introduce a constant distance ϖ_0 defined by $\varpi_0 = h^2/GM$. This is the distance at which an isolated particle in a circular orbit with specific angular momentum h would rotate. From equation (2.1) it is evident that $\nabla p = 0$ at the position given by $\varpi = \varpi_0$, $z = 0$ so that ϖ_0 is also the distance of the density maximum from the rotation axis. Equation (2.8) may then be rewritten as

$$\frac{p}{\rho} = \frac{GM}{(n+1)\varpi_0}\left[\left(\frac{\varpi_0^2}{\varpi^2+z^2}\right)^{1/2} - \frac{1}{2}\left(\frac{\varpi_0}{\varpi}\right)^2 - C'\right], \tag{2.9}$$

where the constant $C' \equiv -C\varpi_0/(GM)$. The zero pressure boundary is given by

$$\left[\left(\frac{\varpi}{\varpi_0}\right)^2 + \left(\frac{z}{\varpi_0}\right)^2\right]^{-1/2} - C' = \frac{1}{2}\left(\frac{\varpi_0}{\varpi}\right)^2 \tag{2.10}$$

The values, $\varpi_\pm$, of ϖ for which the boundary intersects the plane $z = 0$ may be found by putting $z = 0$ and solving the resulting quadratic equation for ϖ_0/ϖ. We obtain

$$\varpi_\pm = \varpi_0/(1 \mp \sqrt{1-2C'})$$

We note that we take ϖ_+ to correspond to the outermost point of the torus and ϖ_- to the innermost. A measure of the distortion, d, of the torus is the dimensionless quantity $d = \tfrac{1}{2}(\varpi_+ + \varpi_-)/\varpi_0$, which is equal to $(2C')^{-1}$. Bounded configurations exist only for $0 < 2C' < 1$. For $2C'$ close to 1, the ring is small and undistorted so that it has nearly circular cross-section. As $2C'$ decreases to zero the torus becomes more and more distended (see Fig. 1). When $2C' = 0$, the innermost point $\varpi_- = \tfrac{1}{2}\varpi_0$ and the outermost $\varpi_+ = \infty$. When $C' < 0$ the configuration extends to infinity and a finite pressure must be supplied at $\varpi = \infty$.

3 The perturbation equation for general polytropic equilibria

The time-dependent equations governing the evolution of the tori discussed in Section 2.1 are the momentum equations, viz.,

$$\frac{\partial v_\varpi}{\partial t} + v_\varpi\frac{\partial v_\varpi}{\partial \varpi} + \frac{v_\phi}{\varpi}\frac{\partial v_\varpi}{\partial \phi} - \frac{v_\phi^2}{\varpi} + v_z\frac{\partial v_\varpi}{\partial z} = -\frac{1}{\rho}\frac{\partial p}{\partial \varpi} - \frac{\partial \psi}{\partial \varpi}, \tag{3.1}$$

$$\frac{\partial v_\phi}{\partial t}+v_\varpi\frac{\partial v_\phi}{\partial \varpi}+\frac{v_\phi}{\varpi}\frac{\partial v_\phi}{\partial \phi}+\frac{v_\varpi v_\phi}{\varpi}+v_z\frac{\partial v_\phi}{\partial z}=-\frac{1}{\rho\varpi}\frac{\partial p}{\partial \phi}-\frac{1}{\varpi}\frac{\partial \psi}{\partial \phi}, \tag{3.2}$$

and

$$\frac{\partial v_z}{\partial t}+v_\varpi\frac{\partial v_z}{\partial \varpi}+\frac{v_\phi}{\varpi}\frac{\partial v_z}{\partial \phi}+v_z\frac{\partial v_z}{\partial z}=-\frac{1}{\rho}\frac{\partial p}{\partial z}-\frac{\partial \psi}{\partial z}, \tag{3.3}$$

where $\mathbf{v}=(v_\varpi, v_\phi, v_z)$ is the velocity, and the continuity equation

$$\frac{\partial \rho}{\partial t}+\frac{1}{\varpi}\frac{\partial}{\partial \varpi}(\rho\varpi v_\varpi)+\frac{1}{\varpi}\frac{\partial}{\partial \phi}(\rho v_\phi)+\frac{\partial}{\partial z}(\rho v_z)=0. \tag{3.4}$$

In addition we assume a polytropic equation of state. To obtain the perturbation equations we linearize the equations (3.1)–(3.4) and write

$$\mathbf{v}=\mathbf{v}_0+\mathbf{v}' \tag{3.5}$$

where

$$\mathbf{v}_0=(0, \varpi\Omega(\varpi), 0) \tag{3.6}$$

is the unperturbed velocity and

$$\mathbf{v}'=(v'_\varpi, v'_\phi, v'_z) \tag{3.7}$$

is the velocity perturbation. We let $p=p_0+p'$ and $\rho=\rho_0+\rho'$, where p', ρ' are the pressure and density perturbations and we recall that p_0 and ρ_0 are functions of ϖ and z only. We drop the subscript zero from now on. By perturbing the equation of state (equation 2.3) we obtain

$$p'/p=\gamma\rho'/\rho. \tag{3.8}$$

Since the unperturbed configuration is axisymmetric, we may Fourier analyse in t and ϕ and write the dependence of the perturbed quantities on t and ϕ in the form $\exp\{i(m\phi+\sigma t)\}$ where m is the azimuthal wavenumber. We take this factor as read in the following analysis. Using this the linearized version of the equations of motion (3.1)–(3.3), combined with equation (3.8) become

$$i(\sigma+m\Omega)v'_\varpi-2\Omega v'_\phi=-\frac{\partial}{\partial \varpi}(p'/\rho), \tag{3.9}$$

$$i(\sigma+m\Omega)v'_\phi+\frac{v'_\varpi}{\varpi}\frac{d}{d\varpi}(\varpi^2\Omega)=-\frac{im}{\varpi}\frac{p'}{\rho}, \tag{3.10}$$

and

$$i(\sigma+m\Omega)v'_z=-\frac{\partial}{\partial z}\left(\frac{p'}{\rho}\right). \tag{3.11}$$

The linearized continuity equation is

$$i(\sigma+m\Omega)\rho'=-\operatorname{div}(\rho\mathbf{v}'). \tag{3.12}$$

It is convenient to define a quantity W such that

$$W = p'/[\rho(\sigma + m\Omega)], \tag{3.13}$$

and to solve equations (3.9)–(3.11) for $\mathbf{v}'$ in terms of W. We find

$$v'_\varpi = i\left(\bar{\sigma}^2 \frac{\partial W}{\partial \varpi} + \frac{\kappa^2 \bar{\sigma} m W}{2\varpi\Omega}\right)\Big/(\bar{\sigma}^2 - \kappa^2), \tag{3.14}$$

$$v'_\phi = \left[-\frac{m\bar{\sigma}^2 W}{\varpi} - \frac{\bar{\sigma}\kappa^2}{2\Omega}\left(\frac{\partial W}{\partial \varpi} + \frac{mW\Omega'}{\bar{\sigma}}\right)\right]\Big/(\bar{\sigma}^2 - \kappa^2), \tag{3.15}$$

and

$$v'_z = \frac{i\partial W}{\partial z}, \tag{3.16}$$

where $\bar{\sigma} = \sigma + m\Omega$ and

$$\kappa^2 = \frac{2\Omega}{\varpi}\frac{d}{d\varpi}(\varpi^2\Omega). \tag{3.17}$$

These equations together with equation (3.8) can be substituted into equation (3.12) to give a single equation for W, which is

$$\frac{D^2}{\varpi}\frac{\partial}{\partial \varpi}\left[\frac{\rho\varpi}{D}\left(\bar{\sigma}^2\frac{\partial W}{\partial \varpi} + \frac{\kappa^2\bar{\sigma}mW}{2\varpi\Omega}\right)\right] + \rho D\left[\frac{m^2 W}{\varpi^2}\left(-\frac{\kappa^2\varpi\Omega'}{2\Omega} - \bar{\sigma}^2\right) - \frac{\kappa^2\bar{\sigma}m}{2\varpi\Omega}\frac{\partial W}{\partial \varpi}\right]$$
$$+ D^2\frac{\partial}{\partial z}\left(\rho\frac{\partial W}{\partial z}\right) + D^2\bar{\sigma}^2\rho^2 w/\gamma p = 0, \tag{3.18}$$

where $D \equiv \bar{\sigma}^2 - \kappa^2$.

Equation (3.18) is a single eigenvalue equation for σ which describes the stability of a polytropic torus with an arbitrary angular velocity distribution. We discuss in Section 4 the particular case of constant specific angular momentum for which $\kappa^2 = 0$. Here we note briefly some general properties of equation (3.18) and of its associated oscillation spectrum.

To illustrate these properties we consider the high wavenumber limit and seek a local dispersion relation by looking for a solution of the form

$$W = W_0 \exp\,[i(k_\varpi \varpi + k_z z)], \tag{3.19}$$

where W_0 is constant, and letting both k_ϖ and k_z tend to infinity while their ratio remains finite (for finite m). In this limit equation (3.18) becomes

$$\rho W_0(Dk_\varpi^2\bar{\sigma}^2 + D^2 k_z^2) = 0 \tag{3.20}$$

which leads to the local dispersion relation

$$\bar{\sigma}^2 = (\sigma + m\Omega)^2 = \kappa^2 k_z^2/(k_z^2 + k_\varpi^2). \tag{3.21}$$

In the limit as k_ϖ and k_z tend to infinity, k_z/k_ϖ can have any value so we may expect the spectrum to be either locally dense or continuous and to cover the range given by

$$-\kappa < \sigma + m\Omega < \kappa \tag{3.22}$$

evaluated for any point in the torus. The arguments given in Appendix A of Papaloizou & Pringle (1982) for the case of uniform rotation can be extended to apply to the Lagrangian formulation of the problem described here. In particular, if any external time dependent force is applied with a frequency in the above range then the Lagrangian displacement becomes unbounded, implying therefore that the oscillation spectrum is indeed either continuous or discrete but locally dense over the above range.

We note further that of course for stability the local dispersion relation given above just requires that

$$\kappa^2 = \frac{2\Omega}{\varpi}\frac{d}{d\varpi}(\varpi^2\Omega) \geqslant 0.$$

This is simply the necessary condition for the stability of a differentially rotating liquid derived by Rayleigh (1916).

4 The perturbation equation and stability criteria for constant specific angular momentum tori

If the torus has constant specific angular momentum, the fact that $\varpi^2\Omega = \text{const.}$ and hence that $\kappa = 0$ simplifies the general perturbation equation (3.18) to

$$\frac{1}{\varpi}\frac{\partial}{\partial\varpi}\left(\rho\varpi\frac{\partial W}{\partial\varpi}\right) - \frac{m^2}{\varpi^2}\rho W + \frac{\partial}{\partial z}\left(\rho\frac{\partial W}{\partial z}\right) = -\frac{\bar{\sigma}^2\rho^2 W}{\gamma p}. \tag{4.1}$$

The feature of equation (4.1) that renders a simple discussion feasible (in contrast to the general case) is that there is no locally dense or continuous portion of the oscillation spectrum, nor is there the possibility of a corotation singularity.

Since Section 4 is, of necessity, somewhat detailed, we briefly review the contents of the section here. In Section 4.1 we demonstrate why finite compressibility is necessary to give rise to instability. This finding is analogous to the results of Broadbent & Moore (1979) who consider the stability of a vortex line and show that it is destabilized by the effect of a finite compressibility. In Sections 4.2–4.4 we turn our attention to a related analogous problem in which the original potential is not just that due to a point mass and in which finite pressure is maintained at the boundaries of the torus. This enables us to use some standard mathematical results. For this problem we show that the eigenvalues are discrete. We demonstrate the existence of some unstable modes and show where and how the stability is lost. We find a criterion for the existence of unstable modes for tori with a central mass point but with finite boundary pressure. The unstable modes are shown to exist provided the boundary pressure is low enough.

The set of unstable tori is infinitely dense in the sense that an unstable configuration exists infinitesimally close to any torus which satisfies the criterion for the existence of unstable modes. The distribution of the unstable modes comes from considering modes of high m and we conclude that the general implication of the analysis for tori with vanishing boundary pressure is that we expect instability at least to modes with arbitrarily large values of m.

In Section 4.5 we draw an analogy with the Klein–Gordon equation and show the relationship between the instability found here and Klein's paradox.

4.1 INTEGRAL CONDITIONS AND THE INFLUENCE OF FINITE COMPRESSIBILITY

In deriving some general integral formulae from equation (4.1) it is convenient to work in

terms of $\sigma_c \equiv \sigma + m\Omega_c$, where Ω_c is a constant angular velocity whose exact value can be specified later at our convenience. Equation (4.1) can now be written as

$$\sigma_c^2 A W + \sigma_c B W + C W = 0 \tag{4.2}$$

where

$$A = \rho^2/\gamma p, \tag{4.3}$$

$$B = 2m(\Omega - \Omega_c)\rho^2/\gamma p, \tag{4.4}$$

and C is the elliptic operator given by

$$CW \equiv \frac{1}{\varpi}\frac{\partial}{\partial \varpi}\left(\rho \varpi \frac{\partial W}{\partial \varpi}\right) + \frac{\partial}{\partial z}\left(\rho \frac{\partial W}{\partial z}\right) + \rho m^2 W\left(\frac{\rho(\Omega - \Omega_c)^2}{\gamma p} - \frac{1}{\varpi^2}\right). \tag{4.5}$$

We now multiply equation (4.2) by $W^* \varpi$, where asterisk denotes complex conjugate, and integrate over the domain in the (ϖ, z) plane occupied by the torus. If the boundary conditions are such that either W or its normal derivative or ρ vanishes at the boundary of the torus we obtain, after integrating by parts,

$$\sigma_c^2 \bar{A} + \sigma_c \bar{B} - \bar{C} = 0, \tag{4.6}$$

where

$$\bar{A} = \int |W|^2 \rho^2 (\gamma p)^{-1} \varpi \, d\varpi \, dz, \tag{4.7}$$

$$\bar{B} = \int |W|^2 2m(\Omega - \Omega_c)\rho^2 (\gamma p)^{-1} \varpi \, d\varpi \, dz, \tag{4.8}$$

and

$$\bar{C} = \int \rho \left[\left|\frac{\partial W}{\partial \varpi}\right|^2 + \left|\frac{\partial W}{\partial z}\right|^2 + |W|^2 m^2 \left(\frac{1}{\varpi^2} - \frac{\rho(\Omega - \Omega_c)^2}{\gamma p}\right)\right] \varpi \, d\varpi \, dz. \tag{4.9}$$

The solution of equation (4.6) is

$$\sigma_c = -\frac{\bar{B}}{2\bar{A}} \pm \left(\frac{\bar{C}}{\bar{A}} + \frac{\bar{B}^2}{4\bar{A}^2}\right)^{1/2}, \tag{4.10}$$

where we note that $\bar{A}$, $\bar{B}$ and $\bar{C}$ are all real. Thus a sufficient condition for stability (real σ_c) is that $\bar{C}$ be positive definite for any W for any choice of Ω_c, and for all values of m. It is evident from equation (4.9) that the only term which could make $\bar{C}$ negative is the one involving ρ/p. In the incompressible limit, in which $\gamma \to \infty$, and provided that p/ρ is non-zero on the boundary, the quantity $\rho(\Omega - \Omega_c)^2/(\gamma p)$ can be made negligibly small compared to $1/\varpi^2$ everywhere in the torus. Thus in the incompressible limit, $\bar{C}$ is positive definite and the system is stable, under the assumed boundary conditions. We conclude that any instability must result from having a finite, rather than an infinite, sound speed.

4.2 THE GENERAL EIGENVALUE PROBLEM

In this section we consider equation (4.1) from a general standpoint and investigate how the complex eigenvalues, that is the unstable modes, arise. However, in order to simplify

the discussion and to make use of a number of standard results we shall find it necessary to consider a wider class of tori than those with just a central point mass. We shall not be able precisely to identify the unstable tori. Nevertheless, the set of unstable tori is dense so that tori with a central point mass are expected to be unstable for some values of the defining parameters (e.g. n, C' or boundary pressure).

To discuss the eigenvalue problem given by equation (4.1) we need to specify boundary conditions on W. For the problem we are considering the appropriate boundary condition is that the density vanishes at the boundary of the torus, and the behaviour of W is then determined by a regularity condition. In order to make use of the many available analytic results, it is more convenient to suppose that the density has some small but finite value at the boundary. We must then specify the behaviour of W there and we consider the cases of either W or its normal derivative vanishing at the boundary. The latter condition corresponds physically to the constraint that the normal component of velocity vanish. We find that our results turn out to be independent of the actual boundary conditions imposed if the density at the boundary is small, and we may therefore expect them to extend to the case where the density vanishes.

The eigenvalue problem given by equation (4.1) can be written

$$L(W) = -(\sigma + m\Omega)^2 \rho^2 W/(\gamma p), \tag{4.11}$$

where L is the linear operator defined by

$$L(W) \equiv \frac{1}{\varpi}\frac{\partial}{\partial \varpi}\left(\rho\varpi \frac{\partial W}{\partial \varpi}\right) + \frac{\partial}{\partial z}\left(\rho \frac{\partial W}{\partial z}\right) - \frac{m^2 \rho W}{\varpi^2}. \tag{4.12}$$

This can be converted to an integral equation by inverting the elliptic operator L. If $L(W) = S$, we may write

$$W = L^{-1}(S)$$

$$= \int G(\varpi, z, \varpi', z')\, S(\varpi', z')\, d\varpi'\, dz' \tag{4.13}$$

where $G(\varpi, z, \varpi', z')$ is a suitable Green's function (e.g. Courant & Hilbert 1953). G has a logarithmic singularity at $\varpi = \varpi'$, $z = z'$ and is therefore square integrable. The eigenvalue problem is therefore equivalent to

$$W + L^{-1}\left(\frac{(\sigma + m\Omega)^2 \rho^2 W}{\gamma p}\right) = 0, \tag{4.14}$$

which is an integral equation for W of the form

$$W + \int K(\varpi, z, \varpi', z', \sigma)\, W(\varpi', z')\, d\varpi'\, dz' = 0 \tag{4.15}$$

where the kernel K is square integrable. This integral equation can be transformed to one with a symmetric kernel and is one to which standard theory can be applied to show that the finite eigenvalues, σ_n, are given by the vanishing of an analytic function $F(\sigma)$ (Courant & Hilbert 1953; Smithies 1965). Accordingly the eigenvalues are discrete and, apart from the possibility of accidental degeneracy, are separated.

We now modify the problem once more to bring the eigenvalue equation into more

standard form. We do so by introducing a parameter α into the right-hand side of equation (4.11), so that it becomes

$$L(W) = -\frac{\alpha^2 m^2 (\nu + \Omega)^2}{\gamma p} \rho^2 W \tag{4.16}$$

where for convenience we work in terms of $\nu \equiv \sigma/m$. The effect of α is to modify the original configuration by scaling the pressure at fixed density. From equation (2.1), we see that to satisfy the equilibrium equation for the unperturbed configuration the introduction of α corresponds to modifying the problem in two respects. First, for example, if the external potential is produced by a point mass we must scale ψ_p by the factor α^2, that is replace ψ_p by ψ_p/α^2. Secondly, the unbalanced centrifugal terms must be accommodated by introducing an appropriately scaled cylindrically symmetric potential that allows rotation at constant specific angular momentum still to occur. The equilibrium configuration so obtained corresponds to a realizable (if not necessarily realistic) configuration which is analogous to the original. The derivation of the perturbation equation (4.1) is not affected by these changes.

By introducing α, and by regarding α rather than ν as the eigenvalue, we obtain an eigenvalue problem to which many standard results can be applied. For real ν, by a slight extension of the integral equation argument, there is a sequence of real discrete α_i ($i = 0, 1, 2, \ldots$) which are the eigenvalues. We shall refer to the solution with $\alpha = \alpha_0$ as the fundamental and to the others as higher modes.

The modes can be derived from maximum–minimum principles applied to the functional

$$V[W] \equiv \frac{\int \rho \left[\left(\frac{\partial W}{\partial \varpi} \right)^2 + \left(\frac{\partial W}{\partial z} \right)^2 + \frac{m^2 W^2}{\varpi^2} \right] \varpi \, d\varpi \, dz}{\int m^2 (\nu + \Omega)^2 \rho^2 (\gamma p)^{-1} W^2 \, \varpi \, d\varpi \, dz} \tag{4.17}$$

For the fundamental mode W_0, $V[W_0] = \alpha_0^2$ is an absolute minimum. For the nth mode W_n, $V[W_n] = \alpha_n^2$ is the minimum obtained by varying W over all trial functions which are orthogonal to all the lower modes $W_i (0 \leqslant i \leqslant n-1)$. The orthogonality condition for two modes W_i and W_j is

$$\int (\nu + \Omega)^2 \rho^2 (\gamma p)^{-1} W_i W_j \, \varpi \, d\varpi \, dz = \delta_{ij} \tag{4.18}$$

assuming the W_i are suitably normalized. We note that since $\rho^2(\nu + \Omega)^2/\gamma p$ is non-zero everywhere except possibly for one value of ϖ, the W_i are a complete set except possibly for a delta-function at that value.

We now investigate how the eigenvalues α_i (assumed positive) depend on ν. We consider initially the case of large $|\nu|$, that is $|\nu| \gg \Omega$, in which case equation (4.16) becomes equivalent to a standard type for the eigenfrequencies of a vibrating membrane with $\nu^2\alpha^2$ as the eigenvalue. For this problem the eigenvalues form a discrete set

$$\nu^2\alpha^2 = \lambda_0, \lambda_1, \lambda_2, \ldots, \lambda_n, \ldots$$

with λ_n real and positive and such that $\lambda_n \to \infty$ as $n \to \infty$. For the moment we can consider just the fundamental mode for which $\alpha^2\nu^2 = \lambda_0^2$ and $\alpha = \alpha_0$. This mode is non-degenerate and the corresponding eigenfunction W does not change sign. For large ν^2, and taking $\alpha_0 > 0$, there are correspondingly two curves in the (α, ν) plane, one for positive ν and one for negative ν, on which $\alpha_0 \to 0$ as $|\nu| \to \infty$. On both of these α_0 increases as $|\nu|$

decreases. If we now go back to the full problem given by equation (4.16) there will be two corresponding curves in the (α, ν) plane. On these $\alpha_0(\nu)$ increases monotonically from close to zero as $|\nu|$ is decreased from large values. We note, however, that as $|\nu|$ is decreased further, α_0 cannot pass through a point in the (α, ν) plane at which $d\alpha_0/d\nu$ is infinite and which would correspond to a minimum in $|\nu|$. For, if this were possible, there would be close to that point two values of α_0 giving a fundamental mode (no nodes in W) for the same value of ν, so contradicting the minimum principle. For the same reason, the two curves $\alpha_0(\nu)$ originating from $\nu = \pm\infty$ cannot cross. We also note that as $|\nu|$ is decreased, $\alpha_0(\nu)$ cannot tend to infinity for some value of ν (recall that Ω is not constant), as this would imply for that value of ν, that the fundamental had infinite eigenvalue. Finally, we note that α_0 cannot be zero for any finite value of ν. We are therefore led to the conclusion that the two curves originating from large $|\nu|$ must coalesce and hence that there is a critical value of $\alpha_0 = \alpha_{0f}$ say, for which $\nu = \nu_{0f}$, above which the fundamental mode cannot be continued for any real ν. At the point of coalescence $\partial\alpha_0/\partial\nu = 0$ and hence, from equation (4.17) we note that

$$\int m^2(\nu_{0f} + \Omega)\,\rho^2(\gamma p)^{-1}\, W_0^2\, \varpi\, d\varpi\, dz = 0. \tag{4.19}$$

We now show that in the neighbourhood of $\alpha = \alpha_{0f}$ there is a solution of equation (4.16) with complex ν. We use linear perturbation theory and, for small $\epsilon > 0$, let $\nu = \nu_{0f} + \epsilon\nu_1 + \epsilon^2\nu_2$, $W = W_0 + \epsilon V_1 + \epsilon^2 V_2$ and $\alpha^2 = \alpha_{0f}^2 + \epsilon\beta_1 + \epsilon^2\beta_2$. Substituting into equation (4.16) and comparing terms of order ϵ gives $\beta_1 = 0$ (using (4.18) and (4.19)) and

$$V_1 = \sum_{n=1}^{\infty} b_n W_n$$

where

$$b_n = \frac{2\nu_1\alpha_{0f}^2}{\alpha_n^2 - \alpha_{0f}^2} \int W_n W_0 (\nu_{0f} + \Omega)\,\rho^2(\gamma p)^{-1}\, \varpi\, d\varpi\, dz \tag{4.20}$$

and we note that $\alpha_n^2 > \alpha_{0f}^2$ for all $n \geqslant 1$.

From the second order terms in ϵ we find that

$$\begin{aligned}\beta_2 &\equiv \epsilon^{-2}(\alpha^2 - \alpha_{0f}^2) \\ &= -\alpha_{0f}^2\nu_1^2\,\mathscr{P}\end{aligned} \tag{4.21}$$

where $\mathscr{P}$ is a positive definite expression. This gives ν_1 and hence ν as a function of α. We conclude that in the neighbourhood of $\alpha = \alpha_{0f}$, for $\alpha < \alpha_{0f}$ the solutions to (4.16) have real values for ν (which we know already) and that for $\alpha > \alpha_{0f}$ the solutions have complex pairs of roots for ν. We have shown, therefore, that stability is lost at this point. We have here used perturbation theory to display explicitly the loss of stability. However, the fact that there are complex roots for ν near $\alpha = \alpha_{0f}$, follows essentially from the fact that the integral equation argument shows that the relation between α and ν is given by the vanishing of an analytic function $f(\alpha, \nu)$. The existence of complex roots near $\alpha = \alpha_{0f}$, $\nu = \nu_{0f}$ can be seen by performing a Taylor expansion about that point.

The argument above was made for the fundamental mode of the associated α problem, for which the nature of the eigenfunction is readily identifiable. An entirely similar argument can be made, however, for each particular eigenmode and corresponding $\alpha_n(\nu)$. There is the additional possible complication of accidental degeneracy but this does not change the essential feature which is that stability must again be lost at some value $\alpha = \alpha_{nf} > \alpha_{0f}$.

Finally we stress that we have *not* proved that unstable modes exist for all real α such that $\alpha > \alpha_{0f}$, but have strictly just proved the existence of instability bands in α close to the values $\alpha = \alpha_{nf}$ ($n = 0, 1, \ldots$). We note further that the above arguments hold, with different values for the α_{nf}, for each value of the azimuthal wavenumber m.

4.3 THE BEHAVIOUR OF THE MODES OF THE RELATED PROBLEM FOR LARGE m

To consider the behaviour for large m, we write the variational expression equation (4.17) in the form

$$V[W] = \frac{\int \frac{\rho W^2}{\varpi} d\varpi\, dz + \frac{1}{m^2}\int \rho\varpi \left[\left(\frac{\partial W}{\partial z}\right)^2 + \left(\frac{\partial W}{\partial \varpi}\right)^2\right] d\varpi\, dz}{\int (\nu + \Omega)^2 \rho^2 (\gamma p)^{-1} W^2 \varpi\, d\varpi\, dz} \tag{4.22}$$

For real ν, the eigenvalues α_i^2 which are extrema of V can be found using the maximum–minimum principles described in the previous section. For large m, the coefficient of the second integral in the numerator, which contains the derivative terms, tends to zero. This means that trial functions can be arbitrarily localized with little effect on V. In the limit as m tends to infinity α_0^2, the absolute minimum of V, is found by localizing the function $\sqrt{\rho}W/\varpi$ at the place in the torus where $(\nu+\Omega)^2\rho\varpi^2/(\gamma p)$ takes its maximum value. If this maximum is $M(\nu)$, then $\alpha_0^2 \to 1/M(\nu)$ as $m \to \infty$. The limiting critical value of α_0^2, α_{0f}^2, is the maximum value, M_0^{-1}, of $M^{-1}(\nu)$ as ν is varied over the real range. Because the influence of the derivative terms on the value of V diminishes as $m \to \infty$, exactly the same argument holds for the higher order modes, because the auxiliary conditions for the minimum problem can be satisfied by a finite combination of non-overlapping localized functions. In particular $\alpha_n^2 \to 1/M(\nu)$ as $m \to \infty$ for all eigenmodes n. It is evident from equation (4.22) that the limiting value approaches $1/M(\nu)$ from above. Thus for each eigenmode n, and given real ν, there is a sequence of values $\alpha_n^2(\nu, m)$ which tend to $1/M(\nu)$ from above as $m \to \infty$. Similarly the critical values $\alpha_{nf}^2(m)$ form a sequence which tend to M_0^{-1} from above as $m \to \infty$. Furthermore from (4.22) we see that as $m \to \infty$, $[\alpha_{nf}^2(\nu, m) - \alpha_{nf}^2(\nu, m+1)]/\alpha_{nf}^2(\nu, m) \sim O(1/m)$.

Given the above, we can now show that the critical values $\alpha_{nf}^2(m)$ are densely packed in the neighbourhood of any value of α such that $\alpha^2 > M_0^{-1}$. To do so choose a large value of m, say m_0. Since $\alpha_{nf}^2(m_0)$ is an increasing function of n we choose n such that $\alpha_{nf}^2(m_0) \gg \alpha^2$. We now consider the corresponding values of $\alpha_{nf}^2(m)$ as m is increased towards infinity. Since $\alpha^2 > M_0^{-1}$, there will be two successive values, m and $m+1$, such that $\alpha_{nf}^2(m) > \alpha^2 > \alpha_{nf}^2(m+1)$ and $m > m_0$. Therefore the distance between these values and the quantity α^2 is less than or of order α^2/m_0. However, m_0 was arbitrary and therefore for any neighbourhood of α^2 there are modes whose critical values $\alpha_{nf}^2(m)$ lie in that neighbourhood. But in Section 4.2 we showed that the critical values are such that for α^2 in their neighbourhood, solutions exist with complex ν. We conclude that any value of α such that $\alpha^2 > 1/M_0$ is arbitrarily close to instability for some mode with sufficiently high m. The set of values of α for which stability occurs is nowhere dense but is not necessarily a set of measure zero (A. Bremner, private communication).

4.4 THE IMPLICATION FOR THE INSTABILITY OF TORI WITH CONSTANT SPECIFIC ANGULAR MOMENTUM

In Section 4.3 we defined $M(\nu)$ as the maximum value of the quantity $(\Omega + \nu)^2\rho\varpi^2/(\gamma p)$

in the torus for a given ν, and showed for $m \to \infty$ that α_{0f}^2 was the reciprocal of the minimum value of $M(\nu)$ for all real ν. Let the torus be situated in the region $\varpi_- \leqslant \varpi \leqslant \varpi_+$. Since $\Omega \propto \varpi^{-2}$ for a constant angular momentum torus, the maximum value of the quantity $F(\nu) = (\Omega + \nu)^2\varpi^2$ for given ν occurs either at $\varpi = \varpi_+$ or at $\varpi = \varpi_-$ depending on the value of ν. It is easy to show that the smallest such maximum value of F occurs for $\nu = -(\Omega_-\varpi_- + \Omega_+\varpi_+)/(\varpi_+ + \varpi_-)$, where $\Omega_\pm$ is the value of Ω at $\varpi_\pm$, respectively, and is equal to $F_{\min} = \varpi_-^2\varpi_+^2(\Omega_- - \Omega_+)^2/(\varpi_+ + \varpi_-)^2$. Furthermore ρ/p increases towards the boundary of the torus and is a maximum at some point on the boundary. If, for example, the boundary is taken to be a constant pressure (or density) surface the maximum value $[\rho/p]_b$ occurs both at $\varpi = \varpi_+$ and at $\varpi = \varpi_-$. We deduce therefore that

$$\alpha_{0f}^2 \geqslant [\gamma p/\rho]_b/F_{\min}$$

$$= \frac{[\gamma p/\rho]_b(\varpi_+ + \varpi_-)^2}{\varpi_+^2\varpi_-^2(\Omega_- - \Omega_+)^2}. \tag{4.23}$$

with equality occurring as $m \to \infty$.

The region in which instability occurs was shown in Section 4.3 to be that in which $\alpha > \alpha_{0f}$. But for tori with a central point mass, which are the main concern of this paper, $\alpha = 1$. Thus for instability of such tori we require

$$\left[\frac{\gamma p}{\rho}\right]_b < \frac{\varpi_+^2\varpi_-^2(\Omega_- - \Omega_+)^2}{(\varpi_+ + \varpi_-)^2}. \tag{4.24}$$

It is evident however that inequality (4.24) is satisfied for tori in which the value of p/ρ on the boundary is much less than the central value, and that we do not require p/ρ to vanish on the boundary.

Indeed, to make the foregoing analysis tractable we have made the assumption that the density took some small, but non-zero, value on the boundary and then imposed boundary conditions on W. In fact, when the density on the boundary is zero (as is the case for the tori we wish to consider), we expect that for finite m the surface boundary conditions should be replaced by a regularity condition on W. From equation (4.1) this condition is seen to be

$$\frac{1}{\rho}\nabla p \cdot \nabla W + (\sigma + m\Omega)^2 W = 0. \tag{4.25}$$

The other properties of the eigenvalue problem can be expected to remain essentially unaltered, and we noted that our arguments about stability do not depend on the form of the boundary condition. This is because when the density vanishes (or nearly vanishes) faster than the normal distance to the boundary, any regular W can be adjusted in a small region near the boundary to satisfy any required boundary conditon without affecting integral forms like $\bar{C}$ in equation (4.9) or $V[W]$ in equation (4.17). We expect that once the boundary density has been reduced below a given value, a given mode will be insensitive to the precise boundary condition imposed. However fundamental modes are sensitive to the boundary values as $m \to \infty$ because they become concentrated near the surface. They change in a way which makes the criterion for stability less easy to satisfy.

We conclude, therefore, that the general implication of inequality (4.24) for the actual tori we wish to consider (for which the boundary density vanishes) is that we expect instability to modes with arbitrarily large values of m.

4.5 ANALOGY WITH THE KLEIN–GORDON EQUATION

We point out here that the occurrence of unstable eigenvalues of ν in equation (4.16) could have been anticipated because the equation is similar to one well known to physicists, namely the Klein–Gordon equation for a particle with wave function ψ, charge e and mass m in an electrostatic field ϕ [note: these definitions of ϕ and ψ apply in this section only and are made to keep in line with familiar quantum mechanical notation]. This equation is (see, for example, Schiff 1955)

$$-c^2\hbar^2\nabla^2\psi + m^2c^4\psi = (E - e\phi)^2\psi, \tag{4.26}$$

where E is the energy eigenvalue, c the velocity of light and $2\pi\hbar$ Planck's constant.

If the particle is confined to a finite region (thus ψ vanishes on the boundary), then, as with the problem discussed above, the eigenvalues are discrete. If ϕ is small, then the eigenvalues for E are real, and take both positive and negative values. It is known (Najman 1983) that if ϕ is increased so that its range exceeds $2mc^2$, then the lowest positive and the highest negative eigenvalues can coalesce producing a complex pair of eigenvalues. This is known as Klein's paradox and is interpreted to mean that particle–antiparticle pairs are produced (Berestetskii, Lifshitz & Pitaevskii 1971).

This phenomenon is identical to the one described above. To be more explicit, let $E = -\alpha\nu$, $\phi = \alpha\Omega/e$ and define the elliptic operator L' to be given by

$$L'(\psi) \equiv -m^2c^4\psi + \hbar^2c^2\nabla^2\psi \tag{4.27}$$

Then equation (4.26) becomes

$$L'(\psi) = -\alpha^2(\nu + \Omega)^2\psi \tag{4.28}$$

This equation is closely analogous to equation (4.16). The elliptic operator L' is slightly different from L but it has identical mathematical properties. Thus the discussion given above in terms of the (α, ν) plane goes through without modification for this case as well.

5 Explicit analytic examples of the instability

The discussion in Section 4 is quite general and leads us to expect instability for constant specific angular momentum configurations. Although the equilibria we considered were for a central Newtonian point mass and a polytropic equation of state, our discussion of stability, and equation (4.1) are quite general and apply for any central potential and for any barotropic equation of state with variable polytropic index n given by $(n+1)/n = d\log p/d\log\rho$. In this section we consider two limiting configurations for which an explicit analytic calculation of the normal modes is possible and which illustrate the nature of the instability.

5.1 THIN CYLINDRICAL SHELL

We consider an equilibrium configuration in which matter is confined to the region $\varpi_0 \leqslant \varpi \leqslant \varpi_0 + a$, with $a \ll \varpi_0$. In this case the pressure and density may take on any constant values. For z-independent modes, equation (4.1) implies for this problem

$$\frac{1}{\varpi}\frac{d}{d\varpi}\left(\varpi\frac{dW}{d\varpi}\right) - \frac{m^2W}{\varpi^2} = -\frac{\bar{\sigma}^2\rho W}{\gamma p}. \tag{5.1}$$

We define a variable $x = \varpi - \varpi_0$ and note that $x \ll \varpi_0$. If we also assume that $m^2/\varpi_0^2 \ll a^{-2}$ and neglect terms of order x/ϖ_0 equation (5.1) becomes

$$\frac{d^2W}{dx^2} = -\frac{\bar{\sigma}^2 \rho W}{\gamma p}. \tag{5.2}$$

If we expand $\bar{\sigma} = \sigma + m\Omega$ about $\varpi = \varpi_0$ for small x we may write the equation in the form

$$\frac{d^2W}{dx^2} = -k^2(\lambda + x)^2 W \tag{5.3}$$

where,

$\lambda = [\sigma + m\Omega(\varpi_0)]/\mu$,

$\mu = -2m\Omega(\varpi_0)/\varpi_0$,

and

$k^2 = \rho\mu^2/(\gamma p)$

are all constants.

For boundary conditions we take $dW/dx = 0$ at $x = 0, a$, although of course a similar analysis with similar conclusions applies to the case of $W = 0$ at the boundaries. Our general discussion of stability given in the preceding section applies here. The quantity k (assumed positive) plays an analogous role to α, with λ being the eigenvalue. The conclusions derived above imply that we expect λ to take on complex values, and so for stability to be lost, when k is sufficiently large. We see that k can be adjusted simply by scaling the constant pressure, with large k corresponding to small pressure, and long sound crossing times. Although there is no z-dependence, we can still apply inequality (4.24) to hold as a criterion for instability to at least high m modes. In this case the inequality becomes $k^2 > 4m^2/(\varpi_0^2 a^2)$. This expectation is somewhat surprising as there is no self-gravity in the problem, and no hint of instability from local analysis (Toomre 1969). This serves to underline the point that local analysis is no reliable guide to instability in the case of nonaxisymmetric modes in shearing systems.

Equation (5.3) is found for example in the asymptotic solution of linear ordinary differential equations with second order turning points (e.g. Nayfeh 1973). The general solution can be written down in terms of Bessel functions in the form

$$W = C_1 F_1(x) + C_2 F_2(x), \tag{5.4}$$

where C_1, C_2 are arbitrary constants and

$F_1(x) = [(x + \lambda)^2]^{1/4} J_{1/4}[\tfrac{1}{2}k(x + \lambda)^2]$,

and

$F_2(x) = [(x + \lambda)^2]^{1/4} J_{-1/4}[\tfrac{1}{2}k(x + \lambda)^2]$.

The occurrence of fractional powers causes no difficulty as they cancel out. We look for solutions in which λ has a small imaginary part, so that $\lambda = \lambda_R + i\delta$, and we assume that $\lambda_R < 0$, but $|\lambda_R| < a$ so that $x + \lambda_R$ changes sign at some point in $0 < x < a$. The boundary condition yields an eigenvalue equation for λ in the form

$$F_1'(0) F_2'(a) - F_2'(0) F_1'(a) = 0. \tag{5.5}$$

Since we anticipate instability for large k, we examine equation (5.5) using asymptotic expansions for the Bessel functions with an error $O(k^{-1})$ which are valid for small δ, including zero. We then find (see, for example, Watson 1944):

$$F_1'(0) \sim -(-\lambda)^{1/2}\left(\frac{4k}{\pi}\right)^{1/2}\sin\left(\frac{k\lambda^2}{2}-\frac{3\pi}{8}\right), \tag{5.6}$$

$$F_1'(a) \sim -(\lambda+a)^{1/2}\left(\frac{4k}{\pi}\right)^{1/2}\sin\left(\frac{k(\lambda+a)^2}{2}-\frac{3\pi}{8}\right), \tag{5.7}$$

$$F_2'(0) \sim +(-\lambda)^{1/2}\left(\frac{4k}{\pi}\right)^{1/2}\sin\left(\frac{k\lambda^2}{2}-\frac{\pi}{8}\right), \tag{5.8}$$

and

$$F_2'(a) \sim -(\lambda+a)^{1/2}\left(\frac{4k}{\pi}\right)^{1/2}\sin\left(\frac{k(\lambda+a)^2}{2}-\frac{\pi}{8}\right). \tag{5.9}$$

We have adopted the convention that the square root with positive real part is to be taken and draw attention to the different signs of these square root terms in equations (5.8) and (5.9). This comes about because $dF_2(x)/dx$ is an odd function of $\lambda + x$ for real values of λ and σ. Substituting (5.6)–(5.9) into (5.5) yields after some elementary algebra

$$\sqrt{2}\sin[\![\tfrac{1}{2}k[\lambda^2+(\lambda+a)^2]]\!] = \cos[\![\tfrac{1}{2}k[\lambda^2-(\lambda+a)^2]]\!]. \tag{5.10}$$

We shall content ourselves by displaying instability by finding solutions of (5.10) for which $\lambda = -\frac{1}{2}a + i\delta$. With this substitution equation (5.10) becomes

$$\cosh(ka\delta) = \sqrt{2}\sin[k(\tfrac{1}{4}a^2-\delta^2)]. \tag{5.11}$$

It is evident that equation (5.11) can have positive (unstable) roots for δ, for particular choices of k. Since our approximations require $ka^2 \gg 1$ and $\delta \ll a$ we may choose $ka\delta$ of order unity so that $1/\sqrt{2}\cosh(ka\delta) = C_0 < 1$. Then k may be chosen so that $\frac{1}{4}ka^2(1-4\delta^2/a^2) = 2N\pi + \sin^{-1}C_0$ for some large integer N. The typical growth rates of instabilities are given by $ka\delta \sim 1$ which give the growth rate

$$-\mathrm{Im}(\sigma) = -\delta\mu \sim \frac{|\mu|}{ka} = \left(\frac{\gamma p}{\rho a^2}\right)^{1/2}. \tag{5.12}$$

Thus the growth times are of order the sound crossing time, implying that the instabilities occur on a dynamical time-scale.

It is instructive to examine the values of k for which we have found instability. For large N these are given by $k = 8\pi N/a^2$. Using the definition of k this corresponds to the quantity

$$q \equiv \left[\frac{\rho}{\gamma p}\right]^{1/2}\frac{2\Omega(\varpi_0)a^2}{\varpi_0} = \frac{8\pi N}{m}. \tag{5.13}$$

If the configurations are defined by lettering a and p/ρ be very small, but such that q has a finite value, then by choosing sufficiently large values of N and m we can ensure that q is arbitrarily close to one of the values for which we have found instability. This implies that any such configuration is such that a slight adjustment of some parameter (e.g. n or p)

is adequate to result in an instability. This is in line with the general discussion given in Section 4.

5.2 THIN ISOTHERMAL RING

We consider a thin isothermal ring under the influence of a central point mass. The ring is concentrated near $\varpi = \varpi_0$ and the equation of state is $p = \rho c_S^2$ where the sound speed c_S is constant. As in Section 5.1 we define a coordinate $x = \varpi - \varpi_0$ and we treat x/ϖ_0 and z/ϖ_0 as small quantities. The integral of the equilibrium equation (2.1) for an isothermal torus is

$$c_S^2 \ln \rho + \psi + h^2/2\varpi^2 = C = \text{constant}. \tag{5.14}$$

The gravitational potential ψ_p (equation 2.2) can be expanded about $\varpi = \varpi_0$, $z = 0$ in the form

$$\psi_p = -\frac{GM}{\varpi_0}\left(1 - \frac{x}{\varpi_0} + \frac{2x^2 - z^2}{2\varpi_0^2} + \ldots\right). \tag{5.15}$$

Similarly

$$\frac{h^2}{2\varpi^2} = \frac{h^2}{2\varpi_0^2}\left(1 - \frac{2x}{\varpi_0} + \frac{3x^2}{\varpi_0^2} + \ldots\right). \tag{5.16}$$

Thus equation (5.14) becomes to second order in x and z,

$$c_S^2 \ln \rho + \left(\frac{GM}{\varpi_0^2} - \frac{h^2}{\varpi_0^3}\right)x - \frac{GM}{2\varpi_0^3}(2x^2 - z^2) + \frac{3h^2x^2}{2\varpi_0^4} = C'' \tag{5.17}$$

where C'' is another constant. As before we specify $h^2 = GM\varpi_0$ and thus obtain

$$\rho = \rho_0 \exp\left(-\frac{GM}{2\varpi_0^3 c_S^2}(x^2 + z^2)\right), \tag{5.18}$$

where ρ_0 is the central density at $x = z = 0$. We note that here (and, of course, close to the density maximum for general constant angular momentum tori) the density contours are concentric circles. As the sound speed, c_S, is decreased the torus becomes more concentrated towards the centre. We define a radial scale length b as $b^2 = c_S^2\varpi_0^3/GM$ and then

$$\rho = \rho_0 \exp\left[-(x^2 + z^2)/2b^2\right]. \tag{5.19}$$

Having set up the equilibrium configuration we can now proceed to the stability analysis. We note first, however, that the configuration is, strictly speaking, unbounded (though of finite mass) and because of this our general discussion given in Section 4 does not straightforwardly apply. In particular in an unbounded system it is possible to have energy escaping to infinity. Note, however, that energy escape does not necessarily act in the direction of stability (Broadbent & Moore 1979). The modes which correspond to this are not square integrable in the sense that neither $\int \rho\, |W|^2 \varpi\, d\varpi\, dz$ nor $\int \rho\, |W|^2 (\sigma + m\Omega)^2 \varpi\, d\varpi\, dz$ exist. As we shall see, apart from modes of this kind, the problem does have some square integrable eigenfunctions for which the above integrals do exist. For such modes a finite boundary at large radius has little effect on the integrals and for them the general theory applies. In particular, unstable modes are found.

To study the stability of the thin isothermal ring we consider equation (4.1) in the limit of small x/ϖ_0 and for $n = \infty$. Using the same notation as for the cylindrical shell problem (section 5.1) we find

$$\frac{\partial}{\partial x}\left(\rho\frac{\partial W}{\partial x}\right)+\frac{\partial}{\partial z}\left(\rho\frac{\partial W}{\partial z}\right)-\frac{m^2\rho W}{\varpi_0^2}=-\rho k^2(x+\lambda)^2\,W \tag{5.20}$$

where in this case

$$k^2=\frac{4m^2\Omega^2(\varpi_0)}{c_S^2\varpi_0^2}=\frac{4m^2}{b^2\varpi_0^2},$$

and

$$\lambda=-\frac{[\sigma+m\Omega(\varpi_0)]\,\varpi_0}{2m\Omega(\varpi_0)}.$$

We have retained the $m^2W\rho/\varpi_0^2$ term here because it can be comparable to the other terms for low order modes which vary on a scalelength b. We now eliminate ρ by using equation (5.19) and obtain the final equation for W:

$$\frac{\partial^2W}{\partial x^2}-\frac{x}{b^2}\frac{\partial W}{\partial x}+\frac{\partial^2W}{\partial z^2}-\frac{z}{b^2}\frac{\partial W}{\partial z}-\frac{m^2W}{\varpi_0^2}=-k^2(x+\lambda)^2\,W. \tag{5.21}$$

We seek a separable solution of the form

$$W=G_1(x)\,G_2(z) \tag{5.22}$$

where $G_1(x)$ and $G_2(z)$ satisfy the equations

$$\frac{d^2G_1}{dx^2}-\frac{x}{b^2}\frac{dG_1}{dx}-\frac{m^2G_1}{\varpi_0^2}-\Lambda G_1+k^2(\lambda+x)^2\,G_1=0 \tag{5.23}$$

and

$$\frac{d^2G_2}{dz^2}-\frac{z}{b^2}\frac{dG_2}{dz}+\Lambda G_2=0, \tag{5.24}$$

where Λ is a separation constant. Equation (5.24) is Hermite's equation for $G_2(z/b)$ and has bounded solutions only if $\Lambda = n_1/b^2$ for $n_1 = 0, 1, 2 \ldots$ The solutions are polynomials of degree n_1.

To solve equation (5.23) we make the transformation

$$G_1(x)=G_3(x)\exp(-\tfrac{1}{2}a_1x^2-a_2x) \tag{5.25}$$

where we choose a_1 and a_2 to satisfy

$$a_1^2+a_1/b^2+k^2=0 \tag{5.26}$$

and

$$a_2=-2\lambda k^2(2a_1+b^{-2})^{-1}. \tag{5.27}$$

These conditions ensure that the coefficient of G_3 is independent of x, and G_3 satisfies

$$\frac{d^2G_3}{dx^2}-\frac{dG_3}{dx}[(2a_1+b^{-2})\,x+2a_2]+G_3(k^2\lambda^2-m^2/\varpi_0^2-n_1/b^2+a_2^2-a_1)=0. \tag{5.28}$$

This is Hermite's equation for G_3 as a function of y, where

$$y = (2a_1 + b^{-2})^{1/2}\left(x + \frac{2a_2}{2a_1 + b^{-2}}\right) \tag{5.29}$$

and has bounded solutions only if

$$k^2\lambda^2 - \frac{m^2}{\varpi_0^2} - \frac{n_1}{b^2} + a_2^2 - a_1 = \left(2a_1 + \frac{1}{b^2}\right)n_2 \tag{5.30}$$

for $n_2 = 0, 1, 2 \ldots$ and the solutions are polynomials in y of degree n_2. For each n_1, n_2 the equations (5.26), (5.27) and (5.30) determine the eigenvalue λ which is linearly related to σ. In solving equation (5.26) for a_1 we note that to have a square integrable eigenfunction we require that $\mathrm{Re}\,(2a_1 + b^{-2}) > 0$. This is possible only if $k^2 < 1/4b^4$. In that case a_1 is real and

$$a_1 = -\frac{1}{2b^2} + \left(\frac{1}{4b^4} - k^2\right)^{1/2}. \tag{5.31}$$

Using this the eigenvalue equation for λ becomes

$$k^2\lambda^2 = (1 - 4k^2b^4)\left[(n_1 - \tfrac{1}{2})\,b^{-2} + \frac{m^2}{\varpi_0^2} + (n_2 + \tfrac{1}{2})\left(\frac{1}{b^4} - 4k^2\right)^{1/2}\right]. \tag{5.32}$$

To obtain unstable modes, we require complex roots for λ and hence the right-hand side of equation (5.32) must be negative. It is evident that a necessary condition for this to occur is that $n_1 = 0$. Thus the unstable modes are independent of z. We recall that $k^2 = 4m^2/(b^2\varpi_0^2)$, so that the criterion for instability becomes

$$2m^2\epsilon^2 + (2n_2 + 1)(1 - 16\,m^2\epsilon^2)^{1/2} < 1 \tag{5.33}$$

where $\epsilon \equiv b/\varpi_0 \ll 1$. If we let $\xi = 16m^2\epsilon^2 = 4k^2b^4$ and note that $0 \leqslant \xi < 1$ the condition becomes

$$2n_2 + 1 < (1 - \tfrac{1}{8}\,\xi)/\sqrt{1 - \xi}. \tag{5.34}$$

If $\xi = 0$, that is $m = 0$, the inequality cannot be satisfied for any n_2. The right-hand side of (5.34) is a monotonically increasing function of ξ which tends to infinity as $\xi \to 1$ from below. Thus as ξ increases from zero to unity, larger and larger values of n_2 (starting with $n_2 = 0$) are able to satisfy the inequality. It is clear from the equations that k^2 plays the same role as did α^2 in the discussion of Section 4, and this result confirms that more and more harmonics go unstable as k^2 is increased. The fastest growth rate clearly occurs for the $n_2 = 0$ mode – the fundamental. If ϵ is sufficiently small that we may treat ξ as a continuous function in the region of interest we find that the fastest growth rate occurs for $m \approx 0.19\,\varpi_0/b$ and is equal to $0.24c_S/b = 0.24\,\Omega(\varpi_0)$. Thus the instability occurs on the dynamical time-scale.

6 Numerical calculation of the eigenfunctions and growth rates

In this section we obtain the eigenfunction with the fastest growth rate, for a given m, for various tori by numerical integration. The equilibrium models we consider are those discussed in Section 2 with a central point mass. We take polytropic index $n = 3$, corresponding to $\gamma = 4/3$, although varying this makes no difference of substance. We consider

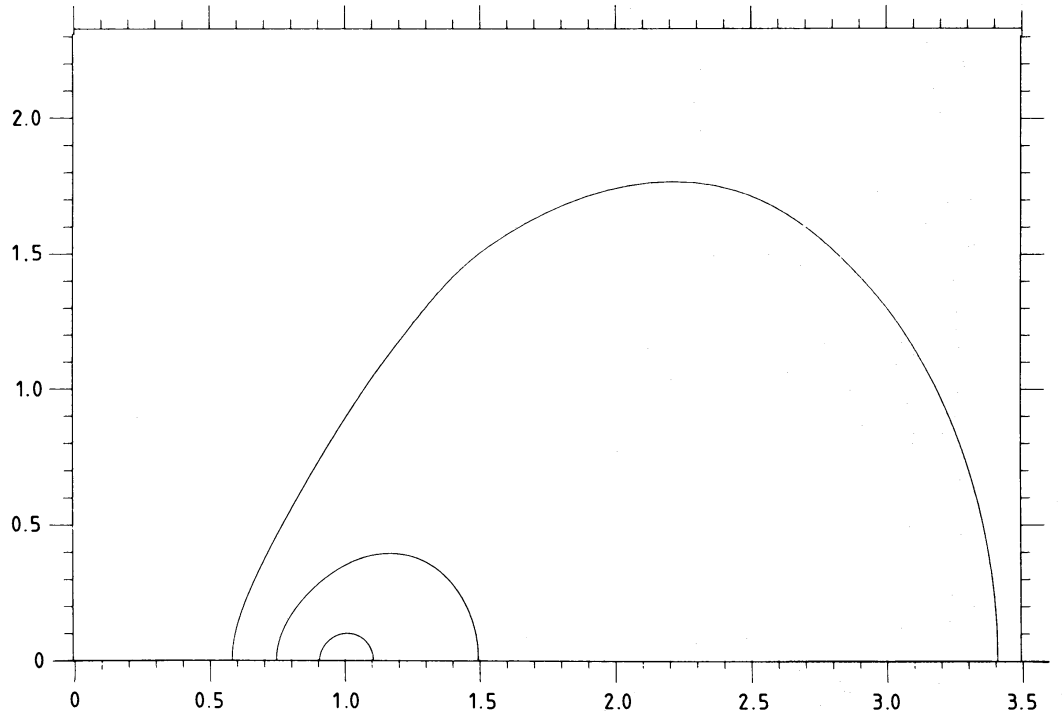

Figure 1. The outer boundaries (zero-density surfaces) of the three tori for which numerical modes were calculated are plotted in the (ϖ, z) plane. The linear dimensions are in units of ϖ_0 so that the density maximum occurs at (1, 0). The tori are symmetric about the $z = 0$ plane and rotate around the $\varpi = 0$ axis. The innermost torus is Model 1, the intermediate, Model 2 and the outermost, Model 3.

three particular models with various values of C', or equivalently distortion parameter d (defined in Section 2) and these are Model 1 ($C' = 0.495$, $d = 1.01$), Model 2 ($C' = 0.444$, $d = 1.125$) and Model 3 ($C' = 0.25$, $d = 2.0$). The shapes of these tori are given in Fig. 1.

The numerical technique employed is to rewrite the eigenvalue equation (4.1) as an initial value problem. This is done by replacing σ by $-(i\partial/\partial t)$ and the equation then becomes

$$\frac{\partial^2 W}{\partial t^2} + 2im\Omega \frac{\partial W}{\partial t} - m^2\Omega^2 W = \frac{\gamma p}{\rho^2} \operatorname{div}(\rho \nabla W). \tag{6.1}$$

This equation is integrated forwards in time from given (arbitrary) initial data using finite difference techniques (see for example Papaloizou & Pringle 1980). The linear initial value problem contains a series of eigenmodes for W, of which the unstable ones are such that $|W|$ grows exponentially in time. In general the initial data is composed of a series of these modes so that if one waits long enough the fastest growing mode dominates the solution. The validity of this technique for determining the fastest growing mode comes about because once this has occurred the spatial structure of the solution is the same as that of an eigenfunction of the original equation (4.1) and the growth rate of $|W|$ is the same as that for that eigenfunction. We shall find that all the tori considered are unstable and that the growth rates are dynamical.

Because of the dangers inherent in looking for exponentially growing solutions in numerical calculations we have done the calculation using two independent methods. The agreement between the methods gives us confidence in the correctness of our results.

6.1 NUMERICAL METHOD A: CARTESIAN GRID

For this we use a Cartesian grid in the (ϖ, z) plane, which is formed in the following way. We divide the line $z = 0$, for which $\varpi_- \leqslant \varpi \leqslant \varpi_+$, into N equal intervals, where usually $N = 49$. We then form a square region in the region $z > 0$ which has the line as one of the sides. Because we expect the eigenfunctions which are symmetric about $z = 0$ (that is $\partial W/\partial z = 0$ on $z = 0$) to grow fastest we impose this as a boundary condition and consider only the region $z \geqslant 0$. The complete square is divided into equal small squares with side-length $\Delta = (\varpi_+ - \varpi_-)/N$. The grid points (ϖ, z) are labelled (i, j). The complete square more than covers the whole torus and points are cut out using the criterion that if $\rho_{i,j}$ is the density at (i, j) and $\rho_{i,j+1}/\rho_{i,j}$ is less than 0.5, $(i, j+1)$ is cut out. The points at $(\varpi_+, 0)$ and $(\varpi_-, 0)$ are also cut out. In this way we avoid excessive density ratios in neighbouring zones and define a boundary to the torus. The densities at the boundary are generally less than 0.1 per cent of the central maximum value. An example of such a grid is given in Fig. 2(a).

Using these coordinates the equation (6.1) is written

$$\frac{\partial^2 W}{\partial t^2} + 2im\Omega \frac{\partial W}{\partial t} = D(W)$$

where

$$D(W) = m^2\Omega^2 W + \frac{\gamma p}{\rho}\left(\frac{\partial^2 W}{\partial \varpi^2} + \frac{1}{\varpi}\frac{\partial W}{\partial \varpi} + \frac{\partial^2 W}{\partial z^2}\right) + \frac{1}{\rho}\left(\frac{\partial p}{\partial \varpi}\frac{\partial W}{\partial \varpi} + \frac{\partial p}{\partial z}\frac{\partial W}{\partial z}\right). \tag{6.2}$$

To proceed to a numerical solution we need to form a finite difference formula for $D(W)$. At grid points for which there are four neighbouring grid points in the torus, this is straightforward and standard (see for example, Potter 1973). For example $(\gamma p/\rho)(\partial^2 W/\partial \varpi^2 + \partial^2 W/\partial z^2)$ is represented at (i, j) by

$$\frac{\gamma p_{i,j}}{\Delta^2 \rho_{i,j}} (W_{i+1,j} + W_{i-1,j} + W_{i,j+1} + W_{i,j-1} - 4W_{i,j}).$$

Complications arise at points near the grid boundaries which lack four neighbours. For these points the first derivatives were represented using the nearest pair of grid points for which a calculation was possible, and forward or backward differences were used if this was necessary. A representation of the second derivative terms was not critical because of the smallness of the coefficient $\gamma p/\rho$ compared to $(\varpi_+ - \varpi_-) \mid \nabla p/\rho \mid$ near the boundary. These were calculated as follows. Suppose the points $(i, j-1)$ and (i, j) were used to estimate $\partial W/\partial z$ at (i, j), those being the nearest for which this was possible, and there was no point at $(i, j+1)$. Then $\partial^2 W/\partial z^2$ was calculated by inserting a fictitious point at $(i, j+1)$ for which $W = W_{i,j}$. This is a very crude treatment. However, tests showed that the same results were obtained even if the term with the $\gamma p/\rho$ factor is ignored. This is because of the smallness of this term and the general insensitivity to the precise boundary conditions for global modes.

To perform the time differencing we rewrite (6.2) as the pair of equations

$$\frac{\partial W}{\partial t} = H, \tag{6.3}$$

$$\frac{\partial}{\partial t}[H \exp(2im\Omega t)] = D(W) \exp(2im\Omega t). \tag{6.4}$$

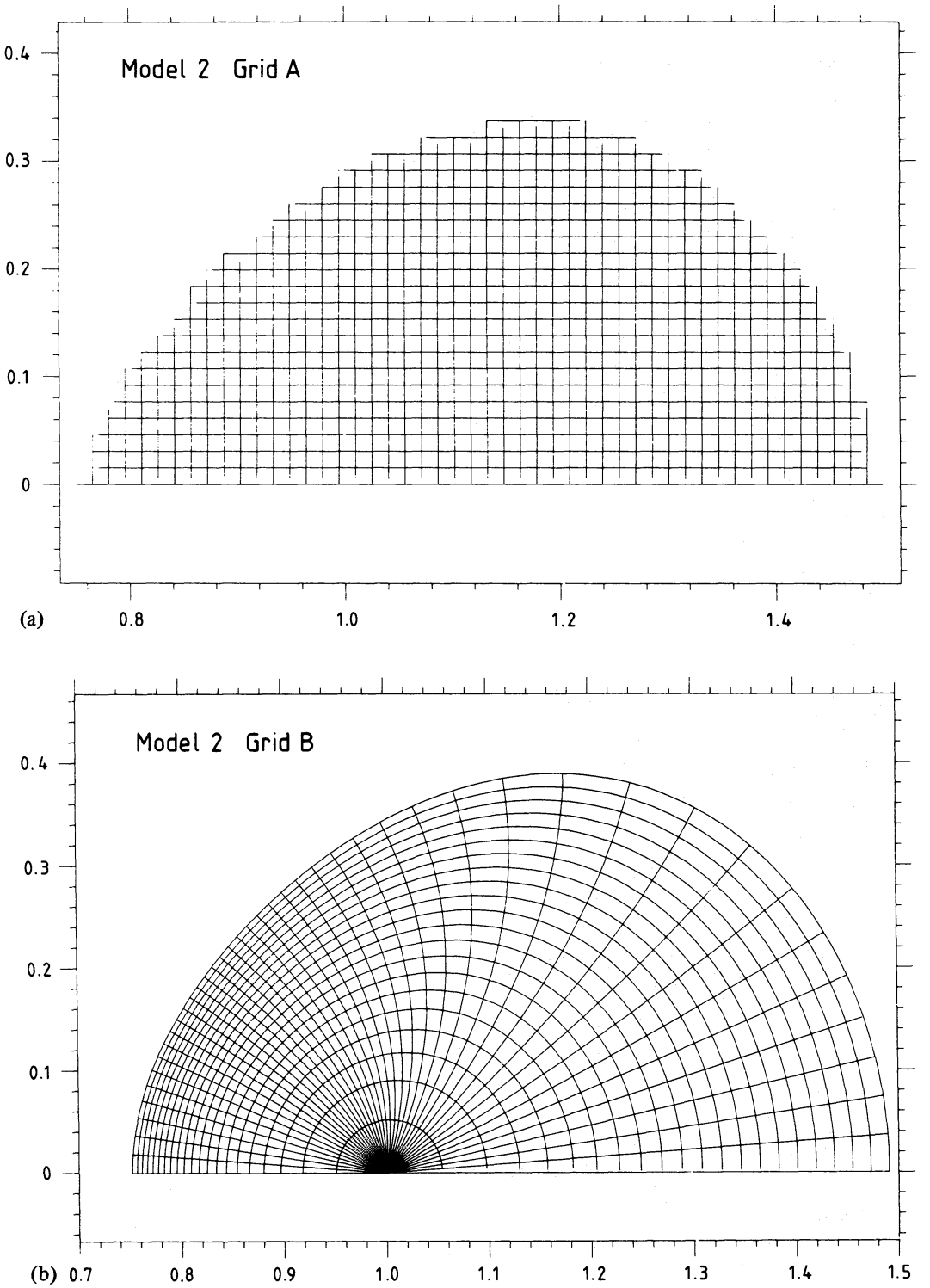

Figure 2. (a) The grid used by numerical Method A for the case of the intermediate torus (Model 2). The axes are in units of ϖ_0. (b) The grid used by numerical Method B for the case of the intermediate torus (Model 2). The axes are in units of ϖ_0.

We define a series of time levels t_n, $t_{n+1/2}$, t_{n+1}, . . . , where the time-step $\Delta t = t_{n+1} - t_n$. We evaluate W at times t_n, t_{n+1}, . . . , and H at times $t_{n+1/2}$, $t_{n+3/2}$, . . . We advance W from t_n to t_{n+1} by using first equation (6.4) to advance H from $t_{n-1/2}$ to $t_{n+1/2}$ and then using equation (6.3). Of course in this method Δt is subject to the usual time-step restric-

tions to ensure stability of the calculation. It must not be longer than the sound crossing time for each zone. We mostly used a time-step equal to half the maximum and tests using a half of this give the same results.

For the particular cases discussed below (Section 6.3) a time of $50-100\,\Omega^{-1}(\varpi_0)$ was sufficient to allow the fastest growing eigenmode to separate out. However, an experiment performed by running Model 2 with $m = 2$ for very long times, showed the emergence of another, probably computational mode, contaminating the initial emergent mode. This could be prevented by the addition of a small diffusive term into the right-hand side of equation (6.2) of the same order as the truncation error associated with the difference equations. This term was of the form

$$C_v \frac{\partial^2 H}{\partial z^2} \frac{(\varpi_+ - \varpi_-)^2}{\Delta t \cdot N^2}$$

where the constant C_v was set equal to 0.037. Checks showed that the properties of the global mode are independent of this term for $C_v \leqslant 0.05$. The emergence of this additional mode is probably associated with the raggedness of the boundary when a Cartesian grid is used. No such emergent mode was found using the method described in Section 6.2.

This raggedness affected the other eigenmodes for $m = 2$ as well but the effects could be eliminated by including the diffusion term (see below).

6.2 NUMERICAL METHOD B: CURVILINEAR GRID

For this method we use a coordinate system of which one coordinate corresponds to the equal density contours. To do this we define a quasi-radial coordinate centred on the density maximum at $(\varpi_0, 0)$.

$$\Psi = \psi_p + \psi_{\text{rot}} + \text{constant}. \tag{6.5}$$

where ψ_p and ψ_{rot} are defined in Section 2 and we adjust the constant to make Ψ zero on the torus boundary. Then $\rho \propto \Psi^n$ and $p \propto \Psi^{n+1}$ where n is the polytropic index. If we define spherical polar coordinates (r, θ) such that $\varpi = r\sin\theta$ and $z = r\cos\theta$ then the curvilinear coordinate orthogonal to Ψ is χ where

$$\tan\chi = \cos\theta/(\cos^2\theta + 1 - \varpi_0/r). \tag{6.6}$$

The coordinate χ is a quasi-angular coordinate and varies from $\chi = 0$ for points with $z = 0$, $\varpi > \varpi_0$ to $\chi = \pi$ for points with $z = 0$, $\varpi < \varpi_0$. The coordinate Ψ varies from Ψ_m at $(\varpi_0, 0)$ to zero at the torus boundary. For eigenfunctions symmetric about $z = 0$ we work in the range $0 \leqslant \chi \leqslant \pi$ and assume $\partial W/\partial\chi = 0$ on $\chi = 0$ and $\chi = \pi$. The grid points are defined by taking points at intervals $\Delta\Psi = \Psi_m/N_\psi$, where usually $N_\psi = 20$, in the Ψ-direction and at intervals $\Delta\chi = \pi/N_\chi$, where usually $N_\chi = 42$ in the χ-direction. We label the point at (Ψ, χ) by (i, j). One of the (Ψ, χ) grids employed is shown in Fig. 2(b).

In this coordinate system we rewrite equation (6.1) in the form

$$\frac{\partial W}{\partial t} = V, \tag{6.7}$$

and

$$\frac{\partial V}{\partial t} = -2im\Omega V + m^2\Omega^2 W + \frac{\gamma p}{\rho^2}\,\text{div}\,(\rho\nabla W). \tag{6.8}$$

In these coordinates the quantity $\mathrm{div}(\rho\nabla W)$ becomes

$$\frac{|\nabla\Psi|\cdot|\nabla\chi|}{\varpi}\left[\frac{\partial}{\partial\Psi}\left(\frac{\rho\varpi|\nabla\Psi|}{|\nabla\chi|}\frac{\partial W}{\partial\Psi}\right)+\frac{\partial}{\partial\chi}\left(\frac{\rho\varpi|\nabla\chi|}{|\nabla\Psi|}\frac{\partial W}{\partial\chi}\right)\right]. \tag{6.9}$$

We perform the spatial differencing in the straightforward way. We evaluate all quantities at the grid points $(i+\frac{1}{2}, j)$ and for example the Ψ-derivative term in $\mathrm{div}(\rho\nabla W)$ at $(i+\frac{1}{2}, j)$ is written as

$$\frac{1}{(\Delta\Psi)^2}\{Q_{i+1,j}[W_{i+3/2,j}-W_{i+1/2,j}]-Q_{i,j}[W_{i+1/2,j}-W_{i-1/2,j}]\},$$

where

$$Q=\frac{\rho\varpi|\nabla\Psi|}{|\nabla\chi|}.$$

The boundary condition at the $\Psi=0$ surface, which is that $\partial W/\partial\Psi=0$ there is taken care of since ρ and hence Q is zero there. The regularity condition on W that $\partial W/\partial\Psi=0$ at $\Psi=\Psi_m$ is easily inserted.

Equations (6.7) and (6.8) are integrated forwards in time using the standard leap-frog method (Potter 1973). As in Method A the time-step must be small enough to ensure computational stability. Tests using half the usual time-step yielded identical results as did tests with double the grid size. For the models discussed below run time in the range $50-100\,\Omega(\varpi_0)^{-1}$ were sufficient to allow the fastest growing eigenmode to separate out.

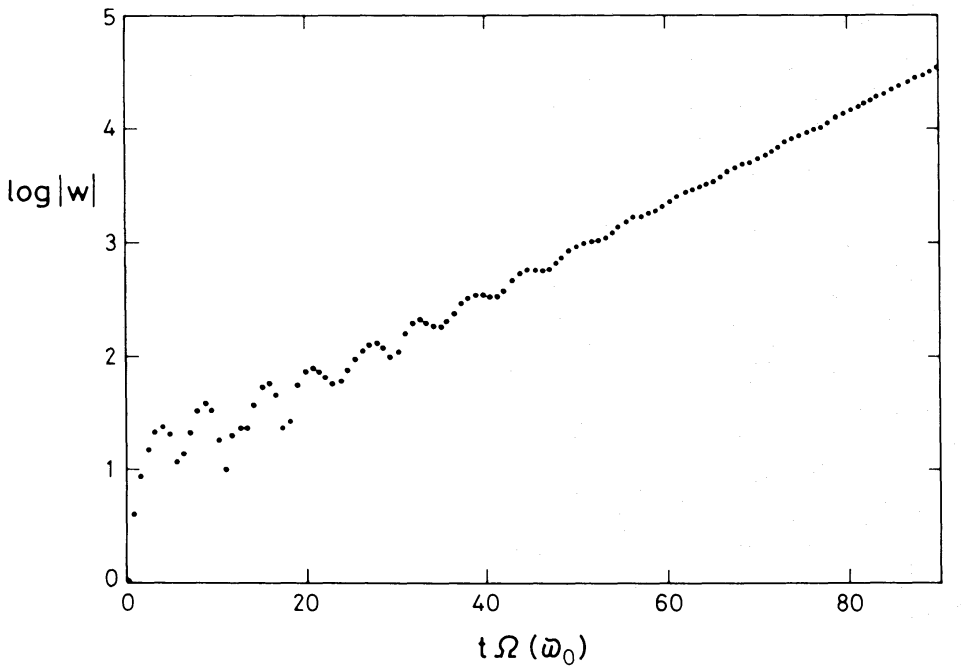

Figure 3. The graph of the maximum value of $|W|$ on the grid against time for the $m=2$ mode of Model 3 using numerical Method B. This illustrates the general behaviour found for $|W|$ as a function of time for all models and both methods. After an initial period of variability the graph settles down onto straight line in the $\log|W|$, t plane and the structure of the mode stabilizes. The growth rate is obtained from the slope of the line.

6.3 COMPUTATIONAL RESULTS

We present results for five particular cases which serve to illustrate the structure of the fastest growing eigenmodes. For each case the equations were integrated forward in time from the initial conditions W = constant and H (Method A) or V (Method B) equal to zero. Varying the initial conditions had no effect on the final outcome. The integration is continued until the normalized distribution of $|W(\varpi, z)|$ stabilizes or, equivalently, until a plot of $\log|W|$ versus time, t, becomes a straight line. At this stage the fastest growing eigenfunction has emerged and the growth time, τ, is obtained from the relation $|W| \propto \exp(t/\tau)$. An example of such a plot is shown in Fig. 3. The five cases we consider are Model 1 with $m = 2$, 4 and 6, Model 2 with $m = 2$ and Model 3 with $m = 2$.

The structures of the eigenmodes are indicated in Figs 4–6. In each figure we plot the contours of $|W|$ and show the result from each numerical method for comparison. Figs

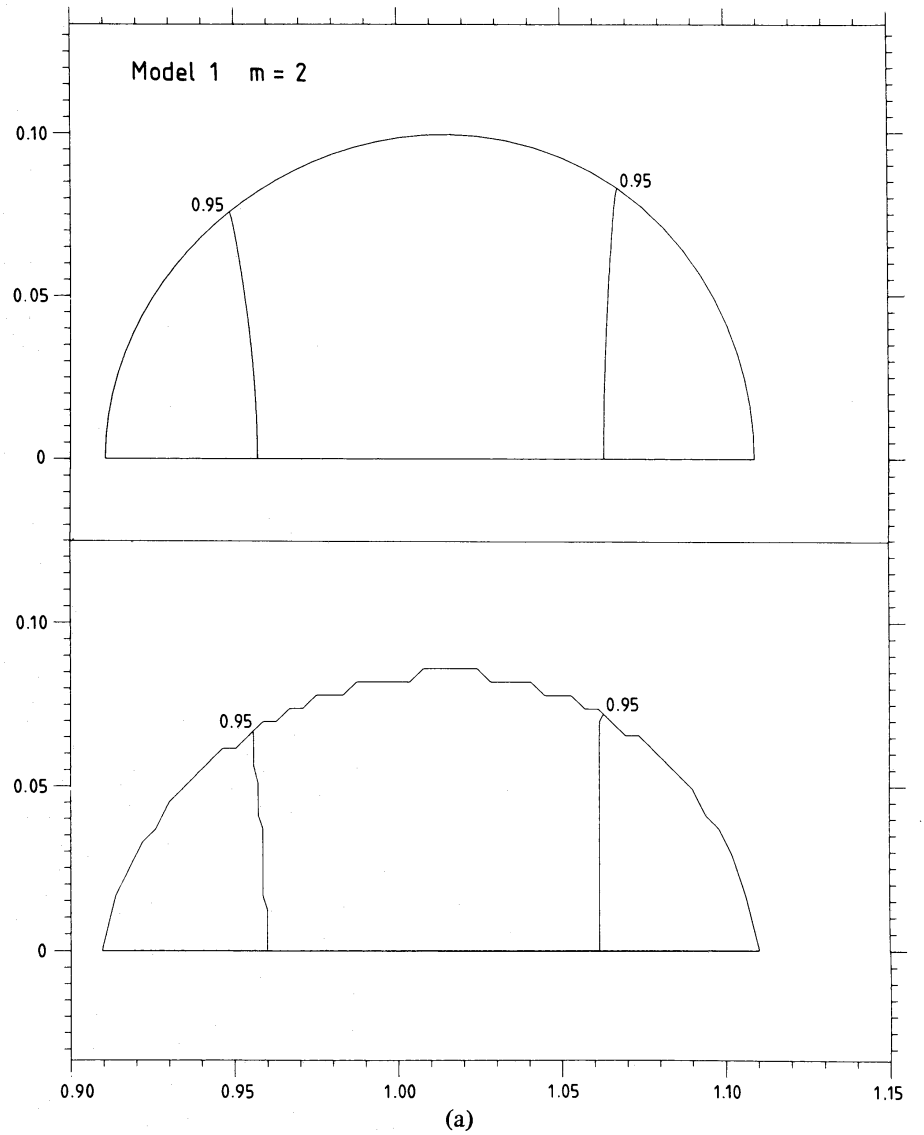

Figure 4. (a) The structure of the fastest growing $m = 2$ eigenmode for the torus Model 1 using numerical Method A (lower) and B (upper). The axes are in units of ϖ_0. The values of the contours are the values of $|W|$, normalized to a maximum value of 1. (b) As for Fig. 4(a) but with $m = 4$. (c) As for Fig. 4(a) but with $m = 6$.

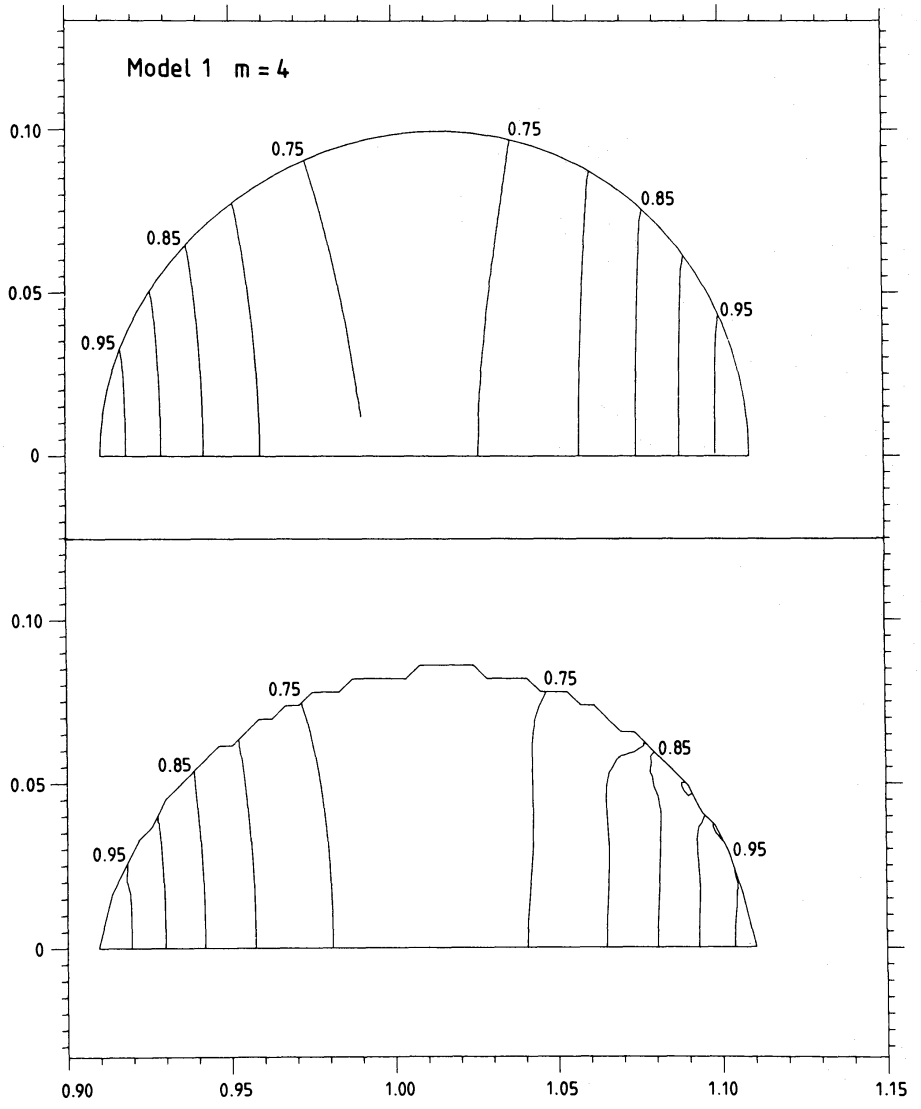

(b)

Figure 4 – *continued*

4(a)–(c) show the modes for the least distorted torus, Model 1, in the cases $m = 2$, 4 and 6 respectively. The mode structure calculated here for a thin ring model with polytropic index $n = 3$ is analogous to that calculated for the $n = \infty$ thin ring in Section 5.2. In particular all the modes have $\partial W/\partial z \approx 0$. The modes are concentrated towards the points $(\varpi_+, 0)$ and $(\varpi_-, 0)$, with the peak value at the latter point, and the concentration becomes greater as m is increased, in line with the high m behaviour found in Section 4. It is evident that the results of the two numerical methods agree reasonably well, at least away from the boundaries where the density is in any case low. In Fig. 5 we show the $m = 2$ eigenmodes for the intermediate case, Model 2. The numerical instability which occurs at the boundary using Method A is illustrated and indeed because of it the peak value of $|W|$ in the plot occurs at a non-zero value of z. The effects of the instability can be completely removed by adding a diffusive term as discussed in Section 6.1. Apart from that the effect of increasing distortion at constant m is to increase the mode concentration towards the edges. The peak value of $|W|$ for this mode occurs at $(\varpi_+, 0)$. Fig. 6 illustrates the effect of increasing the distortion still further and shows the $m = 2$ mode for Model 3. Again the two numerical

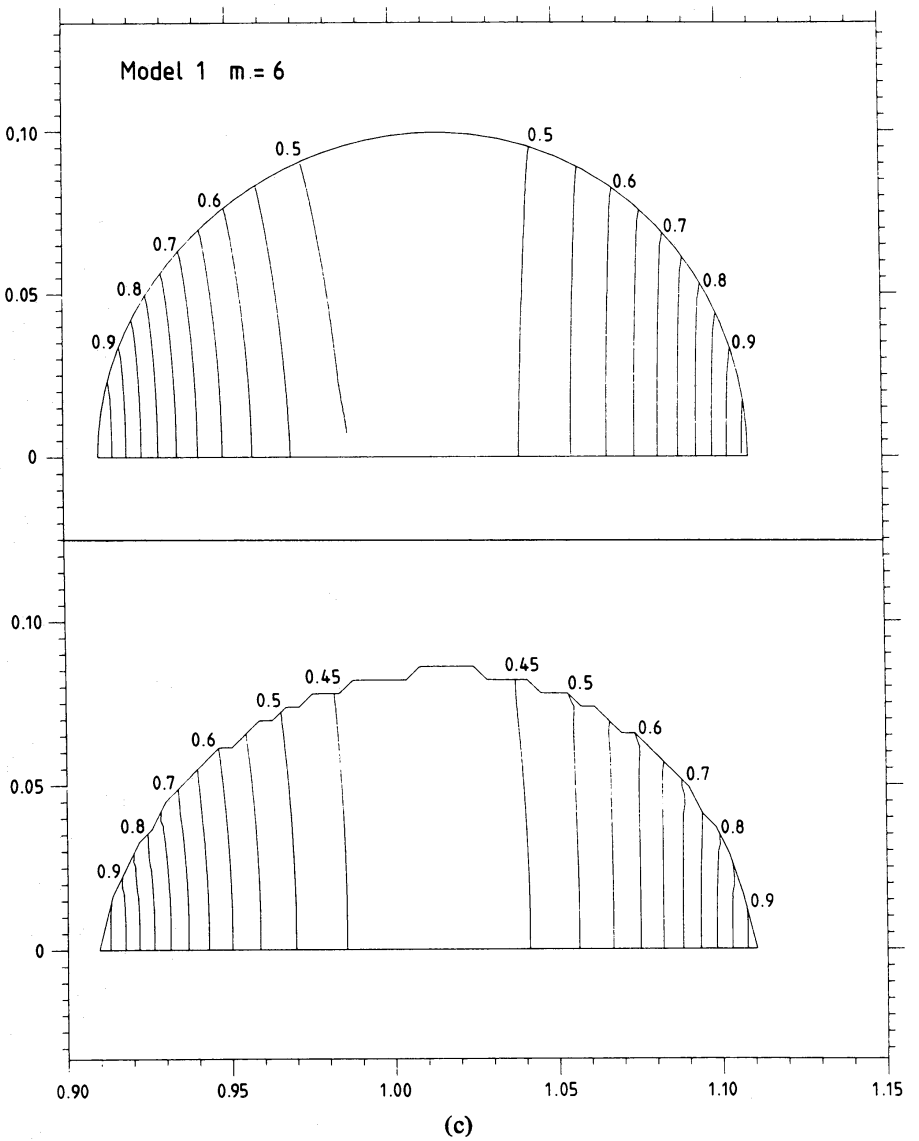

(c)

Figure 4 – *continued*

methods agree reasonably in the region whereas the density is high and the mode is concentrated. For this mode the concentration is high towards the inner edge $(\varpi_-, 0)$. The structure of the mode in the low density outer regions is not well defined due to numerical effects. Apart from the instability already discussed for Method A, the grid used in Method B is significantly distorted in this case in the outer regions.

The growth times obtained for the modes illustrated are given in Table 1 for each numerical method. The growth times are all dynamical in that they correspond approximately to the orbital period $2\pi\Omega(\varpi_0)^{-1}$ for a particle at $(\varpi_0, 0)$.

7 Discussion

We summarize our conclusions as follows:

1. All reasonable models of constant specific angular momentum tori are liable to instability for high m. They are also unstable to low order modes with low m.

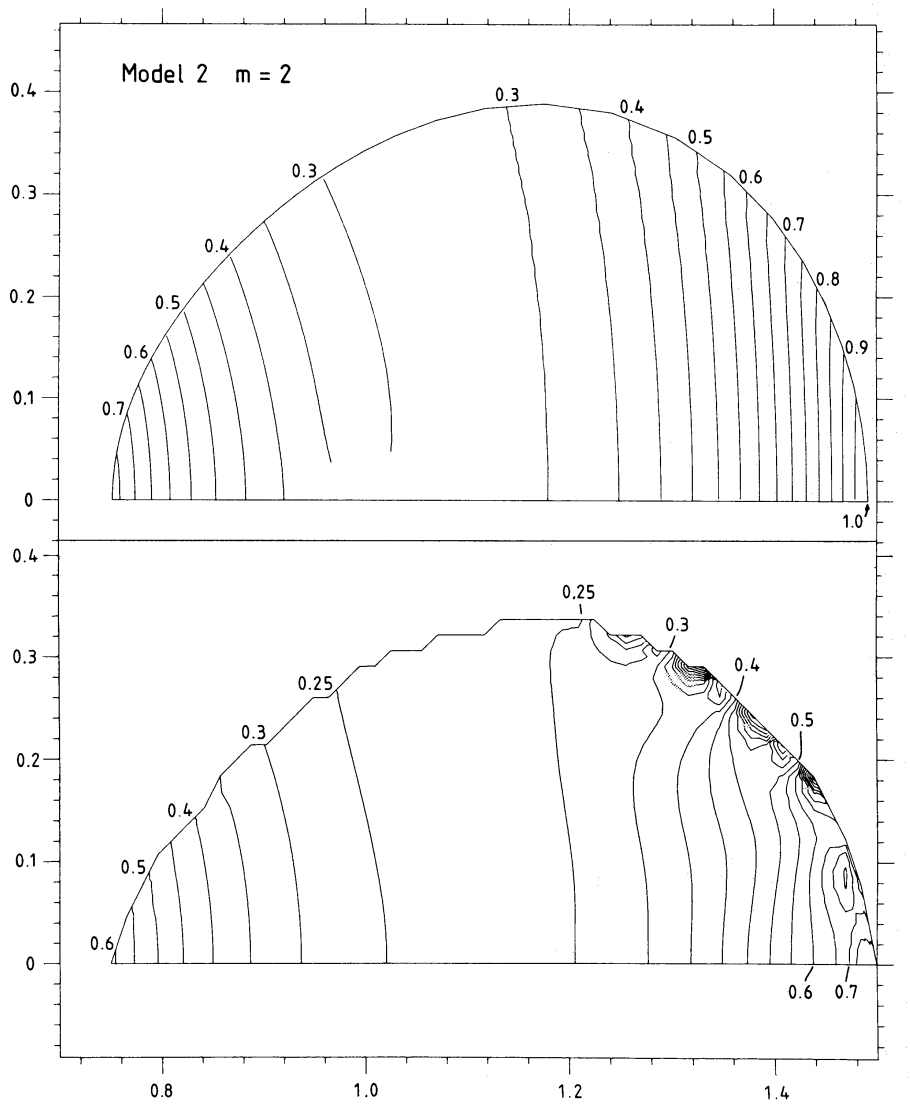

Figure 5. The structure of the fastest growing $m = 2$ eigenmode for the torus Model 2 using Method A (lower) and B (upper). The axes are in units of ϖ_0. The values of the contours are the values of $|W|$ normalized to a maximum value of 1. The effects of the numerical boundary instability in Method A caused by the necessity of treating a ragged boundary are displayed. They have little affect on the solution as a whole and can be removed by the addition of an artificial diffusion term at the edge.

2. The analytical solution for the thin isothermal ring shows that the instabilities persist even though the torus could lose energy to infinity.

3. The instabilities are global. Their existence cannot be deduced from a local analysis nor from consideration of axisymmetric modes. It is the ability of non-axisymmetric modes to transfer angular momentum which enables the tapping of the shear energy and so the growth of the mode.

4. The instabilities are dynamical; their growth times are of order *a* single rotation period or equivalently a single radial sound-crossing time.

These results lead to strong constraints on allowable models of accretion tori. In this regard we note that it is not sufficient to argue that a small change in rotation law or small lack of homentropy will remove the instabilities. The instabilities are global and have dynamical growth times and must persist by continuity arguments if the rotation law or

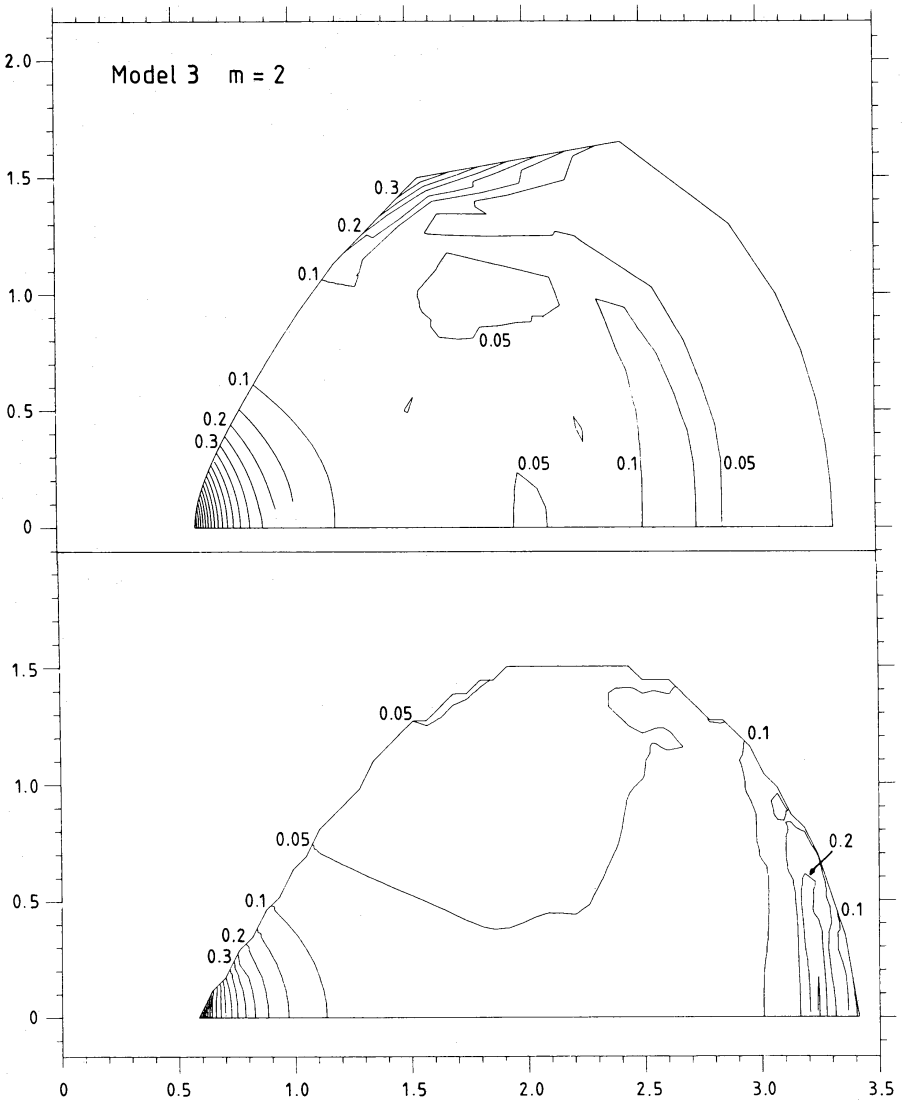

Figure 6. The structure of the fastest growing $m = 2$ eigenmode for the torus Model 3 using Methods A (lower) and B (upper). The axes are in units of ϖ_0. The values of these contours are the values of $|W|$ normalized to a maximum value of 1.

Table 1. Growth times in units of $\Omega(\varpi_0)^{-1}$.

	Method A	Method B
Model 1		
$m = 2$	8.0	8.5
$m = 4$	3.9	4.7
$m = 6$	2.9	4.0
Model 2		
$m = 2$	4.0	4.6
Model 3		
$m = 2$	8.5	10.7

entropy distribution is changed slightly. It is conceivable that they persist even in thin accretion discs and might have relevance to the problem of 'viscosity' or angular momentum transfer within them. We shall address these questions in a subsequent paper.

The results bring into question the viability of models of quasars which involve accretion

tori and of models which require centrifugal force to vacate a funnel up the rotation axis along which jets might originate. The efficiency with which non-axisymmetric perturbations can transfer angular momentum could well preclude the existence of such jet-forming vortex-like regions, by filling them in on the dynamical time-scale. It is clear that further work must be done before these matters can be resolved.

Acknowledgments

We thank Professor J. E. Ffowcs-Williams for bringing the article by Broadbent & Moore to our attention. We thank Dr A. Bremner for discussions about the measure of the set of unstable points in Section 4.3. We thank Dr A. M. Pringle for generating the figures.

References

Abramowicz, M. A., Calvani, M. & Nobili, L., 1980. *Astrophys. J.*, **242,** 772.
Abramowicz, M. A., Henderson, P. F. & Ghosh, P., 1983. *Mon. Not. R. astr. Soc.*, **203,** 323.
Abramowicz, M. A., Livio, M., Piran, T. & Wiita, P. J., 1984. *Astrophys. J.*, in press.
Berestetskii, V. B., Lifschitz, E. M. & Pitaevskii, L. P., 1971. *Relativistic Quantum Theory* (Part 1), Pergamon Press.
Broadbent, E. G. & Moore, D. W., 1979. *Phil. Trans. R. Soc. A,* **290,** 353.
Courant, R. & Hilbert, D., 1953. *Methods of Mathematical Physics,* vols I, and II, Interscience Publishers Inc., New York.
Friedman, J. L. & Schutz, B. F., 1978. *Astrophys. J.*, **222,** 281.
Hacyan, S., 1982. *Astrophys. J.*, **262,** 322.
Kippenhahn, R. & Thomas, H. C., 1978. *Astr. Astrophys.*, **63,** 265.
Lynden-Bell, D., 1978. *Phys. Script.*, **17,** 185.
Madej, J. & Paczynski, B., 1977. *Proc. IAU Coll. No. 42*, p. 313.
Najman, B., 1983. *Proc. Edinburgh Math. Soc.*, **26** (Series II), 181.
Nayfeh, A. H., 1973. *Perturbation Methods,* J. Wiley, New York.
Papaloizou, J. C. B. & Pringle, J. E., 1980. *Mon. Not. R. astr. Soc.*, **190,** 43.
Papaloizou, J. C. B. & Pringle, J. E., 1982. *Mon. Not. R. astr. Soc.*, **200,** 49.
Potter, D., 1973. *Computational Physics,* J. Wiley & Sons.
Pringle, J. E., 1981. *A. Rev. Astr. Astrophys.*, **19,** 137.
Lord Rayleigh, 1916. *Proc. R. Soc. A,* **93,** 143.
Savonije, G. J. & Papaloizou, J. C. B., 1983. *Mon. Not. R. astr. Soc.*, **203,** 581.
Schiff, L. E., 1955. *Quantum Mechanics,* McGraw-Hill.
Shakura, N. I. & Sunyaev, R. A., 1973. *Astr. Astrophys.*, **24,** 337.
Smithies, F., 1965. *Integral Equations*, Cambridge University Press.
Tassoul, J.-L., 1978. *Theory of Rotating Stars,* Princeton University Press.
Toomre, A., 1969. *Astrophys. J.*, **158,** 899.
Toomre, A., 1977. *A. Rev. Astr. Astrophys.*, **15,** 437.
Watson, G. N., 1944. *A Treatise on the Theory of Bessel Functions*, 2nd edn, Cambridge University Press.